

Cite this: *Nanoscale Horiz.*, 2025,  
10, 1025

# Advancements in MOF-based resistive gas sensors: synthesis methods and applications for toxic gas detection†

Linh Ho Thuy Nguyen,<sup>ab</sup> Ali Mirzaei,<sup>c</sup> Jin-Young Kim,<sup>de</sup> Thang Bach Phan,<sup>id</sup><sup>bf</sup>  
Lam Dai Tran,<sup>g</sup> Kevin C.-W. Wu,<sup>id</sup><sup>hij</sup> Hyoun Woo Kim,<sup>\*k</sup> Sang Sub Kim,<sup>id</sup><sup>\*e</sup> and  
Tan Le Hoang Doan,<sup>id</sup><sup>\*bf</sup>

Gas sensors are essential tools for safeguarding public health and safety because they allow the detection of hazardous gases. To advance gas-sensing technologies, novel sensing materials with distinct properties are needed. Metal–organic frameworks (MOFs) hold great potential because of their extensive surface areas, high porosity, unique chemical properties, and capabilities for preconcentration and molecular sieving. These attributes make MOFs highly suitable for designing and creating innovative resistive gas sensors. This review article examines resistive gas sensors made from pristine, doped, decorated, and composite MOFs. The first part of the review focuses on the synthesis strategies of MOFs, while the second part discusses MOF-based resistive gas sensors that operate based on changes in resistance.

Received 25th December 2024,  
Accepted 17th March 2025

DOI: 10.1039/d4nh00662c

rsc.li/nanoscale-horizons

## 1. Introduction to metal–organic frameworks (MOFs)

MOFs are defined by their three-dimensional porous networks, in which inorganic clusters are linked to organic linkers *via* coordination bonds. The flexibility and diversity in the design

of these metal clusters and linkers enable the formation of a wide range of frameworks with varying structures, stability, properties, surface areas, and pore sizes (Fig. 1).<sup>1–3</sup> These exceptional properties of MOFs have enabled their use in a wide range of applications, including clean energy development, greenhouse gas capture (*e.g.*, CO<sub>2</sub>), selective molecular separation from contaminated mixtures, and heterogeneous catalysis in gas or liquid phases.<sup>4–7</sup> Additionally, MOFs with pre-designed structures provide advantages over traditional porous materials and have been assessed for gas-sensing applications in environmental fields.<sup>8–11</sup> MOFs exhibit a range of intriguing properties due to their unique structure and composition.<sup>12,13</sup> Their porous structures have large surface areas, which makes them ideal for gas adsorption,<sup>14</sup> storage,<sup>15</sup> and sensing applications.<sup>16,17</sup> MOFs can be designed with tuneable properties by adjusting their pore sizes, surface functionalities, and chemical reactivity through the selection of specific precursors during synthesis. This tunability also extends to their stability, which provides versatility for applications ranging from catalysis to gas separation.<sup>18–21</sup>

Furthermore, the modular nature of MOFs facilitates the incorporation of various functional groups, which allows for customization for specific applications such as drug delivery in biomedical fields.<sup>22–26</sup> Due to their high porosity and capacity for reversible structural changes, MOFs are promising candidates for sensing and controlled release systems.<sup>27–29</sup> Their unique electronic and magnetic properties further extend their utility to fields such as electronics and magnetism.<sup>30,31</sup>

<sup>a</sup> Faculty of Pharmacy, University of Health Sciences, Ho Chi Minh City 70000, Vietnam

<sup>b</sup> Vietnam National University, Ho Chi Minh City 70000, Vietnam.  
E-mail: dlhtan@inomar.edu.vn

<sup>c</sup> Department of Materials Science and Engineering, Shiraz University of Technology, Shiraz 71557-13876, Iran

<sup>d</sup> The Research Institute of Industrial Science, Hanyang University, Seoul, 04763, Republic of Korea

<sup>e</sup> Department of Materials Science and Engineering, Inha University, Incheon 22212, Republic of Korea. E-mail: sangsub@inha.ac.kr

<sup>f</sup> Center for Innovative Materials and Architectures (INOMAR), Ho Chi Minh City 70000, Vietnam

<sup>g</sup> Institute of Materials Science, Vietnam Academy of Science and Technology, Hanoi 11300, Vietnam

<sup>h</sup> Molecular Science and Technology Program, Taiwan International Graduate Program, Academia Sinica, Taipei 11529, Taiwan

<sup>i</sup> Department of Chemical Engineering and Materials Science, Yuan Ze University, Chung-Li, Taoyuan 32003, Taiwan

<sup>j</sup> Department of Chemical Engineering, National Taiwan University, Taipei 10617, Taiwan

<sup>k</sup> Division of Materials Science and Engineering, Hanyang University, Seoul 04763, Republic of Korea. E-mail: hyounwoo@hanyang.ac.kr

† Congratulations to Vietnam National University Ho Chi Minh City on its 30th Anniversary (1995–2025).

Consequently, the diverse and tunable properties of MOFs drive extensive research and innovation, establishing them as a cornerstone in materials science and engineering.

Gas sensors are essential for enhancing safety and awareness by detecting toxic and dangerous gases.<sup>32</sup> While traditional gas sensing technologies are effective, there is an ongoing need for novel sensing materials that offer improved performance. Due to their porosity and distinctive chemical features, MOFs hold great promise for gas-sensing applications.<sup>33,34</sup> MOFs' high surface areas and significant porosity enhance gas adsorption, which leads to measurable changes in electrical resistance. These sensors also benefit from the chemical tunability

of MOFs, which allows for customization to detect specific gases by modification of their metal nodes and linkers. Advances in synthesis methods, such as solvothermal, microwave irradiation, and mechanochemical methods, have enabled the creation of MOFs with tailored properties for enhanced gas-sensing performance.<sup>35</sup> The integration of MOFs into resistive sensors has expanded their applications to fields including industrial safety, environmental monitoring, and healthcare diagnostics.<sup>36</sup> This review explores advancements in MOF-based resistive gas sensors, focussing on synthesis strategies and their performance in detecting various gases.

*Linh Ho Thuy Nguyen obtained her BS (2013) and MSc (2017) degrees from the University of Science, Vietnam National University, Ho Chi Minh City (VNU-HCM). She later earned her PhD from the same institution in 2023 and is now a lecturer at the Faculty of Pharmacy, University of Health Sciences, VNU-HCM. Her research interests include the synthesis, functionalization, and applications of metal-organic frameworks (MOFs).*

*Ali Mirzaei received his PhD degree in Materials Science and Engineering from Shiraz University in 2016. He was a visiting student at Messina University, Italy, in 2015 and from 2016 to 2018, he was accepted as a postdoctoral fellow at Hanyang University in Seoul. He is the author or co-author of more than 130 peer-reviewed papers. Currently, he is an assistant professor of materials science and engineering at Shiraz University of Technology, Iran. He is interested in the synthesis and characterization of nanocomposites for gas sensing applications.*

*Jin-Young Kim received his B.S. degree from Inha University, Republic of Korea, in 2017. He is currently working as an integrated course candidate at Inha University, Republic of Korea. He has been working on 1-dimensional oxide nanowires and 2-dimensional transition metal dichalcogenide gas sensors.*

*Bach Thang Phan is an Assoc. Professor at Center for Innovative Materials and Architectures (INOMAR), a member of Vietnam National University in Ho Chi Minh city. He received his PhD degree from Sungkyunkwan University, Korea, in 2009. His research interests include the synthesis and applications of nanostructural materials for memristor, thermoelectric conversion, drug delivery, biosensors and gas sensors.*

*Lam Dai Tran is currently the Director of the Institute for Tropical Technology, Vietnam Academy of Science and Technology (VAST). He graduated with a bachelor's degree in Solid and Semiconductor Chemistry from the Faculty of Chemistry, Belarusian State University, in 1994; and he received his PhD degree in Surfaces-Intersurfaces Chemistry from the University of Paris VII Denis Diderot (France) in 2003. He was appointed as Associate Professor of Chemistry in 2009 and as Professor of Chemistry in 2018. Currently, the main research directions of Prof. Tran are inorganic chemistry, nanomaterials and biomaterials.*

*Kevin C.-W. Wu got his PhD degree at The University of Tokyo in 2005. After that, he was a post-doc at Waseda Univ. with Prof. Prof. Kazuyuki Kuroda in Japan and at Iowa State Univ. with Prof. Victor Lin in USA from 2005 to 2008. He is currently a professor at the Dept. Chem. Eng., National Taiwan University (NTU), Taiwan. He has published more than 160 international journal papers with a total citation over 7400 times (h index 46). In 2018, he was selected as a Humboldt scholar from Humboldt Foundation, Germany, and received an outstanding research award from the Ministry of Science and Technology (MOST), Taiwan. He is serving as an editor for three SCI journals (Advanced Powder Technology, Scientific Reports and Journal of the Taiwan Institute of Chemical Engineers) and is an editorial board member for two prestigious international journals (ACS Sustainable Chemistry & Engineering (ACS) and Applied Catalysis B: Environmental (Elsevier)). His research interests include the design and synthesis of functional nanoporous materials for sustainable chemistry and engineering applications including biomass conversion, membrane separation, biomedicine and energy devices.*

## 2. Synthesis of MOFs

MOF synthesis involves combining inorganic ions or clusters with organic bridges under controlled conditions to form a three-dimensional porous network. This process requires meticulous control over several critical parameters to tailor the structural and functional properties of the resulting MOFs.<sup>4,37,38</sup> The choice of the metal precursor and organic ligand is fundamental, as it dictates the composition and properties of the MOF.<sup>39–41</sup> The solvent and solvothermal conditions, including temperature and pressure, affect the thermodynamics and kinetics of the reaction, which alters crystal growth and morphology.<sup>42–45</sup> Furthermore, maintaining optimal pH levels is essential to control the stability of metal ions and ligand deprotonation.<sup>46</sup> The reaction temperature, duration, and concentration of reactants are crucial in determining the rate of MOF formation and the properties of the final product.<sup>47,48</sup> Templates or modulator agents can influence crystal growth, while mechanochemical synthesis parameters, such as milling time and speed, affect energy input and MOF formation.<sup>49–51</sup> Careful consideration and control of these parameters enable the fine-tuning of MOF synthesis, ensuring reproducibility and customization of diverse applications. Moreover, various synthesis methods offer distinct advantages and disadvantages, influencing the final properties of the material (Table 1).

---

*Hyoun Woo Kim joined the Division of Materials Science and Engineering at Hanyang University as a full professor in 2011. He received his B.S. and M. S. degrees from Seoul National University and his PhD degree from Massachusetts Institute of Technology (MIT) in electronic materials in 1986, 1988, and 1994, respectively. He was a senior researcher in Samsung Electronics Co., Ltd. from 1994 to 2000. He has been a professor of materials science and engineering at Inha University from 2000 to 2010. He was a visiting professor at the Department of Chemistry of Michigan State University, in 2009. His research interests include gas sensors.*

---

*Sang Sub Kim joined the Department of Materials Science and Engineering, Inha University, in 2007 as a full professor. He received his B.S. degree from Seoul National University and his M.S and PhD degrees from Pohang University of Science and Technology (POSTECH) in Material Science and Engineering in 1987, 1990, and 1994, respectively. He was a visiting researcher at the National Research in Inorganic Materials (currently NIMS), Japan, for 2 years each in 1995 and in 2000. In 2006, he was a visiting professor at the Department of Chemistry, University of Alberta, Canada. In 2010, he also served as a cooperative professor at Nagaoka University of Technology, Japan. His research interests include the synthesis and applications of nanomaterials such as nanowires and nanofibers, functional thin films, and surface and interfacial characterization, for application in gas sensors.*

Commonly used synthesis techniques include hydrothermal, solvothermal, microwave, ionothermal, pyrolysis, mechanochemical, electrochemical, and template-directed synthesis (Fig. 2). Solvothermal and mechanochemical synthesis methods are among the most promising routes for industrial-scale production of MOFs. Solvothermal synthesis offers tunable reaction conditions and is already used for large-scale applications, while mechanochemical synthesis is a green, solvent-free approach with excellent scalability and energy efficiency. Microwave-assisted synthesis also shows potential due to its rapid reaction times and reproducibility, though the equipment limitations may affect large-scale implementation. The selection of a synthesis technique depends on the desired MOF features, scalability, and the intended application.<sup>42,52</sup> Researchers are continually exploring innovative approaches to enhance the efficiency, reproducibility, and sustainability of MOF synthesis techniques.<sup>53,54</sup>

### 2.1. Hydrothermal synthesis

Hydrothermal synthesis is widely used for preparing MOFs, providing precise control over the formation of well-defined crystalline structures. In this method, metal salts and organic linkers are combined in a high-temperature/high-pressure aqueous solution, typically within an autoclave. The hydrothermal environment promotes the dissolution of reactants, accelerates their interaction, and fosters the nucleation and growth of MOFs.<sup>55</sup> Controlled conditions, including temperature, pressure, and synthesis time, play important roles in determining the final size, morphology, and properties of the resulting MOFs.<sup>56</sup> In addition, hydrothermal synthesis is advantageous for producing MOFs with enhanced crystallinity and purity, which improves structural integrity and performance in various applications. This method is also valuable for generating MOFs with tailored functionalities, making it a versatile tool for MOF synthesis for gas sorption,<sup>57</sup> catalysis,<sup>58</sup> and drug delivery.<sup>52</sup>

### 2.2. Solvothermal synthesis

Solvothermal synthesis is a prominent technique for MOF fabrication and it utilizes organic solvents under controlled

---

*Tan Le Hoang Doan received his B.S. degree in honor program from the University of Science, Viet Nam National University – Ho Chi Minh City in 2009 and his PhD degree in Molecular and Nanoarchitecture program from Viet Nam National University – Ho Chi Minh City in 2017. He was a postdoctoral researcher at Kyoto University, Japan, in 2018. He is currently working as a senior researcher at Center for Innovative Materials and Architectures (INOMAR), Viet Nam National University – Ho Chi Minh City. His research interests include the design, synthesis, and applications of porous materials.*

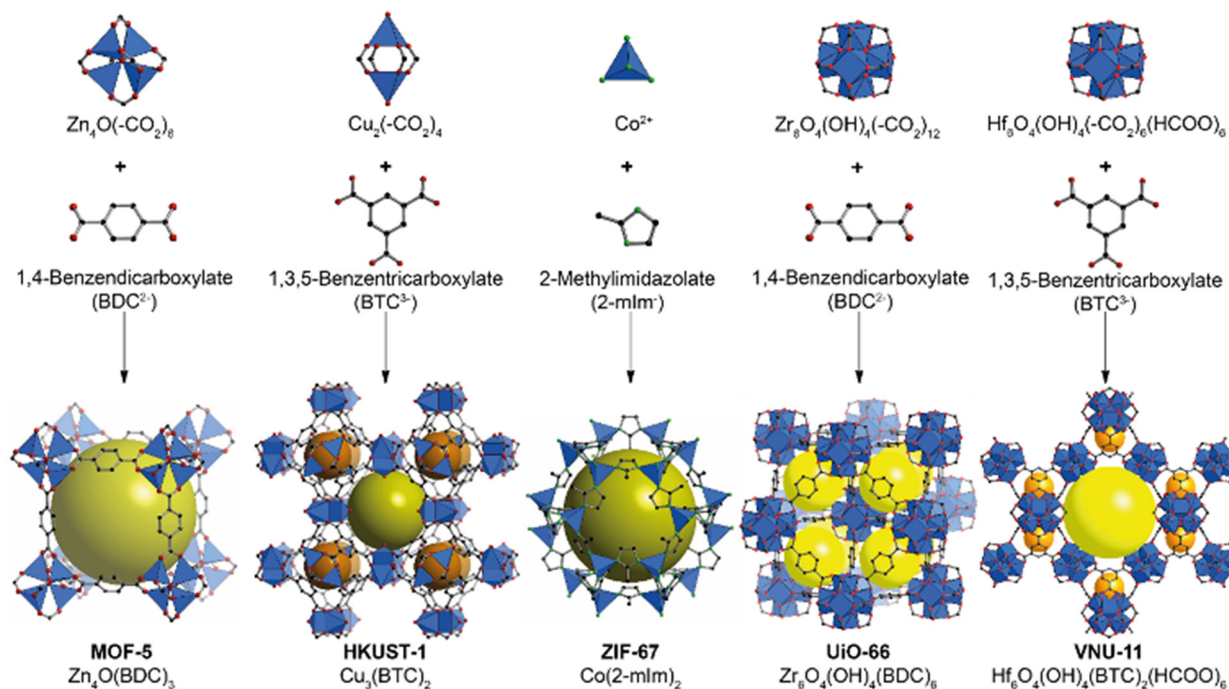


**Fig. 1** Schematic representation of the synthesis of various metal–organic frameworks (MOFs) through the self-assembly of metal clusters with organic linkers, resulting in distinct structural and functional properties. MOF-5 ( $\text{Zn}_4\text{O}(\text{BDC})_3$ ) and UiO-66 ( $\text{Zr}_6\text{O}_4(\text{OH})_4(\text{BDC})_6$ ) utilize 1,4-benzenedicarboxylate ( $\text{BDC}^{2-}$ ) ligands. HKUST-1 ( $\text{Cu}_3(\text{BTC})_2$ ) and VNU-11 ( $\text{Hf}_6\text{O}_4(\text{OH})_4(\text{BTC})_6(\text{HCOO})_6$ ) incorporate 1,3,5-benzenetricarboxylate ( $\text{BTC}^{3-}$ ). ZIF-67 ( $\text{Co}(\text{2-mlm})_2$ ) features  $\text{Co}^{2+}$  nodes and 2-methylimidazole ( $\text{2-mlm}^-$ ) linkers, forming a stable zeolitic framework.

**Table 1** Comparison of general advantages and limitations of MOF synthesis techniques

Synthesis technique	Advantages	Disadvantages
Hydrothermal synthesis	<ul style="list-style-type: none"> <li>Controlled conditions result in well-defined MOFs</li> <li>Enhanced crystallinity and purity</li> <li>Versatile for various MOF compositions</li> </ul>	<ul style="list-style-type: none"> <li>Requires high-temperature and pressure equipment</li> <li>Limited scalability</li> </ul>
Solvothermal synthesis	<ul style="list-style-type: none"> <li>Tunable synthesis conditions in organic solvents</li> <li>Flexible reaction parameters</li> <li>Suitable for scalable production</li> </ul>	<ul style="list-style-type: none"> <li>Solvent dependence and potential toxicity</li> <li>Longer reaction times compared to hydrothermal</li> </ul>
Microwave synthesis	<ul style="list-style-type: none"> <li>Rapid heating reduces reaction times</li> <li>Improved reproducibility</li> <li>Energy-efficient compared to conventional methods</li> </ul>	<ul style="list-style-type: none"> <li>Equipment limitations for large-scale production</li> <li>Limited control over local temperature variations</li> </ul>
Ionothermal synthesis	<ul style="list-style-type: none"> <li>Enhanced stability of MOFs</li> <li>Unique properties due to ionic liquid medium</li> <li>Potential for direct integration in devices</li> </ul>	<ul style="list-style-type: none"> <li>Limited availability and cost of ionic liquids</li> <li>Limited scalability</li> </ul>
Pyrolysis synthesis	<ul style="list-style-type: none"> <li>Simple and energy-efficient</li> <li>No need for solvents</li> <li>Applicable under harsh conditions</li> </ul>	<ul style="list-style-type: none"> <li>Potential for MOF decomposition at high temperatures</li> <li>Limited control over morphology</li> </ul>
Mechanochemical synthesis	<ul style="list-style-type: none"> <li>Green, solvent-free synthesis</li> <li>Short reaction times</li> <li>Scalable and energy-efficient</li> </ul>	<ul style="list-style-type: none"> <li>Limited control over reaction selectivity</li> <li>Potential for contamination from milling equipment</li> </ul>
Electrochemical synthesis	<ul style="list-style-type: none"> <li>Direct integration onto conductive substrates</li> <li>Accurate control over MOF properties</li> <li>Applicable in electrocatalysis and energy storage</li> </ul>	<ul style="list-style-type: none"> <li>Limited control over MOF size and morphology</li> <li>Requires specific electrode materials and setups</li> </ul>
Template-directed synthesis	<ul style="list-style-type: none"> <li>Controlled morphology and properties</li> <li>Tailored MOFs for specific applications</li> <li>Enhanced reproducibility</li> </ul>	<ul style="list-style-type: none"> <li>Template removal can be challenging</li> <li>Limited versatility with some template systems</li> </ul>

temperature and pressure conditions. In this method, organic ligands and metal salts react within closed systems filled with an organic solvent rather than water.<sup>59</sup> Moreover, the choice of solvent is vital as it affects the solubility of the reactants and the resulting MOF characteristics. The solvothermal conditions enable fine-tuning of the reaction kinetics, which allows the

production of MOFs with tailored structures, sizes, and functionalities.<sup>60</sup> In addition, using organic solvents for solvothermal synthesis offers flexibility, which enables researchers to manipulate the reaction parameters and obtain the desired properties.<sup>61</sup> This method is valuable for developing MOFs with enhanced porosity, surface area, and stability, making them

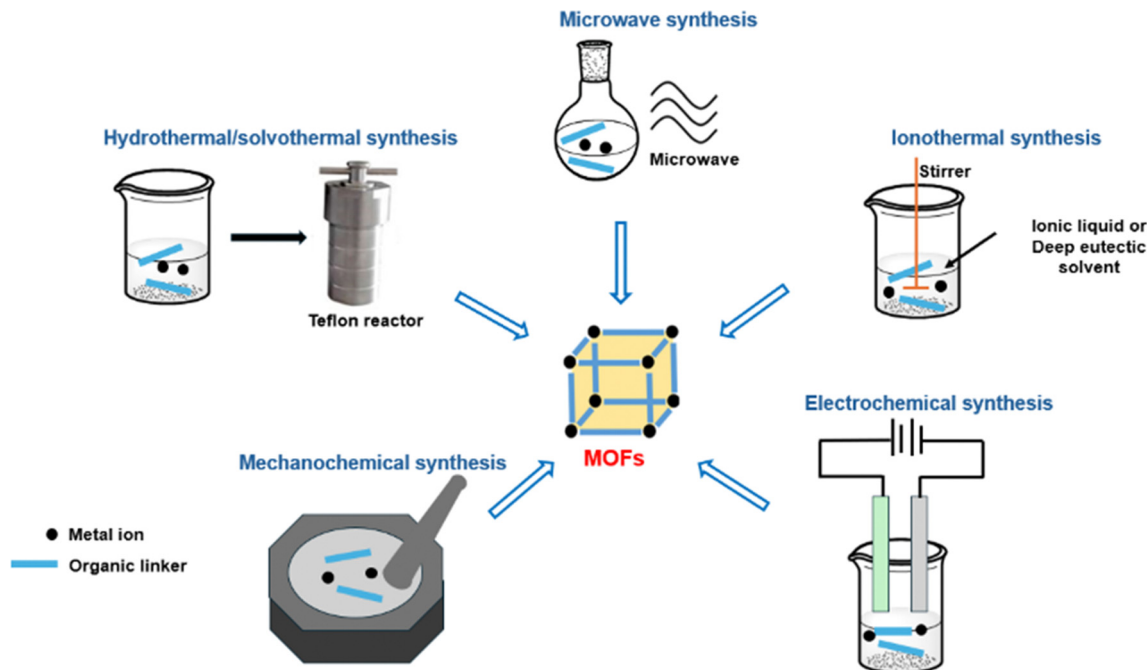


Fig. 2 Representative synthesis methods for MOFs, highlighting different approaches for assembling metal ions (black dots) and organic linkers (blue lines) into highly porous structures.

well-suited for gas storage and sensing,<sup>62,63</sup> catalysis,<sup>64,65</sup> and separation processes.<sup>66,67</sup> The versatility and controllability of solvothermal synthesis contribute to its widespread adoption for synthesizing MOFs with diverse compositions and properties.

### 2.3. Microwave synthesis

Microwave synthesis is an efficient and fast method for producing MOFs. This technique involves exposing the precursors to microwave radiation, which rapidly heats the reaction mixture.<sup>68</sup> The localized and uniform heating provided by microwaves accelerates the reaction kinetics, which results in shorter synthesis times compared to conventional methods. Microwave synthesis offers several advantages, including improved reproducibility, enhanced purity, and high yields.<sup>69</sup> The controlled heating also minimizes side reactions, which leads to MOFs with well-defined structures.<sup>70,71</sup> This method is advantageous due to its energy efficiency and scalability, which makes it an attractive option for MOF production.<sup>72</sup> In addition, microwave synthesis is effective in tailoring the size, morphology, and porosity of MOFs, which enhances their versatility for applications such as gas adsorption,<sup>73,74</sup> drug delivery,<sup>75</sup> and sensing.<sup>76,77</sup> Microwave synthesis of MOFs offers rapid crystallization and energy efficiency, often yielding materials with comparable or even enhanced crystallinity compared to that achieved with conventional methods. However, the resulting morphology can be varied and sometimes finer or irregular particles form due to rapid nucleation and growth. While there may be trade-offs in porosity or defect formation, careful optimization of reaction parameters can mitigate these issues, ensuring high-quality MOFs within a significantly reduced synthesis time.<sup>78</sup> The combination

of speed, efficiency, and tunability makes microwave synthesis a valuable tool for the production of advanced MOF materials.

### 2.4. Ionothermal synthesis

Ionothermal synthesis is a distinctive method for producing MOFs utilizing ionic liquids as reaction solvents and templating agents. Metal salts and organic ligands react within the ionic liquid medium, where the exceptional properties of ionic liquids—such as low volatility and high thermal stability—are important in defining the characteristics of the resulting MOFs.<sup>79</sup> The ionothermal conditions provide an alternative to conventional solvents, which results in MOFs with enhanced stability and unique structural features. Ionic liquids serve as both the reaction medium and template, which affect crystal growth and morphology.<sup>80–82</sup> Moreover, the tailored properties of MOFs synthesized *via* ionothermal routes make them attractive for gas adsorption, catalysis, and environmental applications.<sup>83,84</sup> This synthesis technique highlights the significance of the reaction environment in shaping the final characteristics of MOFs, providing a valuable route for the synthesis of advanced MOFs with tailored features.

### 2.5. Pyrolysis synthesis

Pyrolysis synthesis offers a distinctive and unconventional route for producing MOFs, where metal–organic complexes are subjected to high temperatures in the absence of oxygen, which leads to the thermal decomposition of the precursors and the subsequent formation of MOFs.<sup>85</sup> Pyrolysis induces a controlled and rapid thermal transformation that forms MOFs with unique structures and properties. The absence of oxygen prevents both oxidation and combustion reactions and

preserves the MOF framework. Pyrolysis synthesis is advantageous due to its simplicity and efficiency, often producing MOFs with enhanced thermal stability and well-defined crystalline structures.<sup>86</sup> This method is particularly useful in applications where traditional solution-based approaches may be problematic.<sup>87,88</sup> Pyrolysis is an efficient strategy for the scalable or controlled synthesis of MOFs, as it can leverage high temperatures without compromising the integrity of the MOF structure.

### 2.6. Mechanochemical synthesis

Mechanochemical synthesis is an innovative and sustainable method for producing MOFs. This technique uses mechanical energy, usually generated by ball milling, to induce chemical reactions between solid-state reactants, including metal salts and organic linkers. The grinding action in mechanochemical synthesis helps break chemical bonds and promotes the intimate mixing of precursors, which leads to the formation of MOFs. This method offers several advantages, including reduced reaction times, increased yields, and the elimination of solvents, which makes it environmentally friendly.<sup>89,90</sup> The simplicity of this approach enables straightforward scalability and enhances energy efficiency. In addition, mechanochemical synthesis allows for control over particle size and morphology, which can help tailor the characteristics of the MOFs. The green and sustainable attributes of this method, coupled with its ability to produce MOFs with unique features, position it as a promising method for efficient and environmentally friendly MOF fabrication.<sup>91</sup>

### 2.7. Electrochemical synthesis

Electrochemical synthesis is a powerful and versatile approach to synthesize MOFs. Metal ions and organic linkers undergo electrochemical reactions within a conductive solution or on an electrode surface. Metal ions are reduced at the cathode and subsequently react with organic linkers to form MOFs.<sup>92</sup> The applied electrochemical potential serves as a driving force for the formation of MOFs, which enables control over the growth and deposition of the framework. Furthermore, this method offers advantages, such as tunable synthesis conditions, which facilitate the manipulation of MOF properties such as size, morphology, and crystallinity.<sup>93,94</sup> In addition, electrochemical synthesis allows for the direct integration of MOFs onto conductive substrates, which enables their use in electrocatalysis,<sup>95–97</sup> sensing,<sup>98</sup> gas and liquid separation,<sup>99</sup> and energy storage devices.<sup>100</sup> The ability to tailor the MOF properties through electrochemical control, combined with its eco-friendly characteristics and potential for direct integration into electronic devices, makes electrochemical synthesis a promising approach for advancing MOF applications in various technological fields.

### 2.8. Template-directed synthesis

Template-directed synthesis is a strategic and controlled method that can be used for producing MOFs, where pre-existing templates or sacrificial agents guide the formation of the desired crystalline structures. This innovative approach allows researchers to manipulate the nucleation and growth of MOFs and target

specific morphologies and properties. The chosen template (often an auxiliary molecule or framework) serves as a mold that imparts its characteristics onto the growing MOF structure.<sup>101</sup> The template is removed after synthesis, leaving behind a thoroughly tailored MOF. This technique is especially valuable for applications that demand exact control of MOF features such as pore size and functionality.<sup>102–105</sup> Furthermore, template-directed synthesis enables the engineering of MOFs with targeted properties and enhances their utility in various areas, including gas separation, catalysis, and drug delivery. This is done by ensuring the reproducibility and customization of these materials for specific applications.<sup>106–109</sup>

The synthesis of MOFs for resistive gas sensors is a critical process that impacts the performance of the sensors directly. Several advanced synthesis techniques have been developed to create MOFs with tailored properties, increasing their suitability for gas sensing applications.<sup>110</sup> In addition, each method can be fine-tuned to produce MOFs with specific surface areas, porosity, and chemical functionalities, which are essential for achieving high sensitivity and selectivity in resistive gas sensors.<sup>111</sup> These tailored MOFs are subsequently incorporated into sensor devices, where their ability to adsorb gas molecules alters the electrical resistance and enables effective gas detection.<sup>112</sup>

## 3. Functionalization of MOFs

The functionalization of MOFs is a vital aspect that enhances their versatility and tailors their properties for certain applications. MOF functionalization involves the introduction of additional chemical groups or functionalities to the MOFs, affecting surface chemistry, porosity, and reactivity. The MOF functionalization can introduce minor structural changes, but well-controlled approaches such as post-synthetic modification (PSM), metal site functionalization, and surface grafting help preserve their integrity and porosity. PSM allows the incorporation of functional groups without disrupting the framework, while metal site functionalization enhances reactivity, and surface grafting prevents pore blockage while maintaining a high surface area. Careful selection of functional groups and optimization of synthesis conditions minimize any reduction in porosity, ensuring MOFs remain effective for gas detection applications.<sup>113,114</sup> The following section reviews several common strategies that are used for functionalizing MOFs.

### 3.1. Post-synthetic modification (PSM)

PSM involves introducing functional groups or ligands into existing MOFs after their synthesis. Nguyen *et al.* reported a novel Zr-MOF, MOF-700, for methane storage.<sup>115</sup> The group employed post-synthesis metalation with various copper salts to produce an isorecticular series of MOFs with enhanced volumetric methane storage capacities. As a result, MOF-701 showed a 50% enhancement compared to the parent MOF-700 (Fig. 3).<sup>116</sup> Moreover, amine-functionalization on ZIF-11 could be performed after the synthesis using 2-aminobenzimidazole,

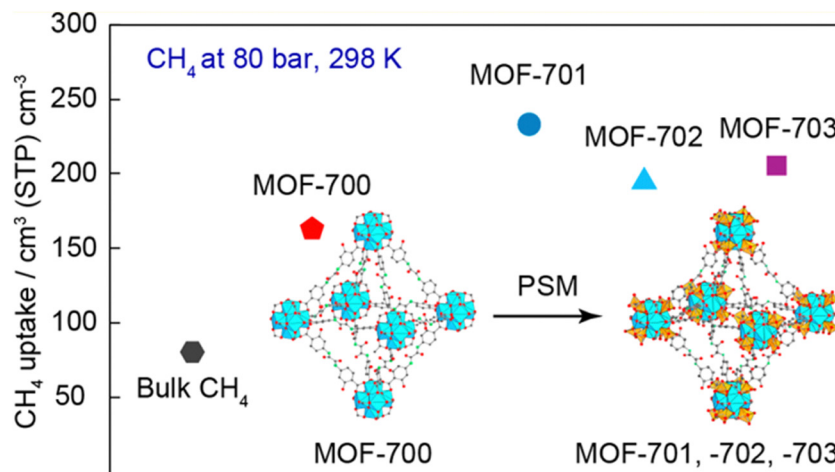


Fig. 3 The enhancement of methane uptake in MOFs through PSM. The graph presents  $\text{CH}_4$  adsorption capacities at 80 bar and 298 K, comparing the initial MOF-700 structure with its modified derivatives MOF-701, MOF-702, and MOF-703. The structural representations show the transformation of MOF-700, where PSM introduces additional functional groups (highlighted in orange), potentially enhancing gas adsorption properties.<sup>115</sup> Reproduced from ref. 115 with permission from The American Chemical Society, copyright 2022.

which improved the stability in aqueous media and generated fluorescent nanoparticles, highlighting its possible application as a marker material for detecting copper ions.<sup>117</sup> In other words, PSM allows precise control of the type and amount of functionalization while minimizing the impact on the overall structure and improving the MOF activity.<sup>118</sup>

### 3.2. Functionalization of metal sites

Tailoring the metal sites within an MOF structure by replacing or modifying metal ions can endow the material with unique reactivity or selectivity. This strategy is particularly advantageous for catalytic applications.<sup>119–122</sup> Moreover, through the sulfation of an Hf-MOF, sulfate groups were attached to an Hf-oxo cluster, which then acted as an effective heterogeneous catalyst for heterocyclization in benzoxazole preparation (Fig. 4).<sup>119</sup> In addition, modulator-mediated functionalization on the metal cluster can provide a versatile platform to improve the separation capability of MOF membranes, which is exemplified by producing mixed-matrix membranes with high  $\text{CO}_2$  separation yields.<sup>120</sup> Also,  $\text{Eu}^{3+}$  ions were introduced to produce a luminescent  $\text{Eu}^{3+}$ @Ni-MOF composite with high sensitivity and selectivity to aspartic acid, highlighting its potential as a sensitive luminescent probe for detecting aspartic acid.<sup>121</sup>

### 3.3. Incorporation of functional linkers

During MOF synthesis, selecting specific linkers with desired functionalities allows for the creation of a functionalized MOF from the outset. This approach integrates functional groups into the framework during its formation.<sup>123–125</sup> An examination of the adsorption mechanism of indole on Zr-MOFs (specifically Zr-BDC-NH<sub>2</sub> and Zr-BDC-NO<sub>2</sub>) showed that linker-functionalized Zr-MOFs exhibit enhanced indole adsorption capacities *via* their hydrogen and  $\pi$ -hydrogen bonds (Fig. 5).<sup>123</sup> The presence of functional groups can induce splitting of the  $\pi$  orbital of the linker. In addition, the specific functional groups can cause a

half-metal-to-insulator transition in the ferromagnetic configuration of the host material.<sup>125</sup>

### 3.4. Coordinative unsaturation

Certain MOFs feature unsaturated metal sites, which enable the addition of ligands and functional groups. This method can also enhance the binding affinity for specific molecules or facilitate catalytic processes.<sup>126–128</sup> Furthermore, defect-engineered MOFs (called UiO-66-NH<sub>2</sub>-X) were synthesized with controlled structural defects induced by an acetic acid modulator. This revealed a switch-on effect for photocatalysis with a volcano-type trend in the  $\text{H}_2$  generation rate, where Pt@UiO-66-NH<sub>2</sub>-100 showed the highest activity (Fig. 6).<sup>128</sup>

### 3.5. Surface functionalization

Modifying the external surface of MOFs can improve their interaction with specific molecules. Common surface functionalization methods include grafting, chemical derivatization, or the introduction of reactive groups.<sup>117,129–131</sup> The tobacco mosaic virus (TMV) has been utilized as a robust protein template to control the morphology of MOFs. This approach resulted in rod-like TMV@MOF core-shell structures (C-S) with tunable diameters (Fig. 7). The synthetic conditions affected its stability and allowed the chemical modification of the virus particle beneath the MOF shell, which indicated mass transportation inside the MOF shell.<sup>117</sup> Moreover, a fluorescent organosilica coating named ZIF-8@BPMO was applied to nano ZIF-8 to enhance bio-interactions and reduce flocculation.<sup>131</sup>

### 3.6. Encapsulation of functional molecules

Incorporating functional molecules or nanoparticles into the pores of MOFs can provide additional functionalities, such as guest molecule adsorption or controlled release.<sup>133,134</sup> Homogeneous porous ZIFs, with particle sizes below 100 nm, serve as

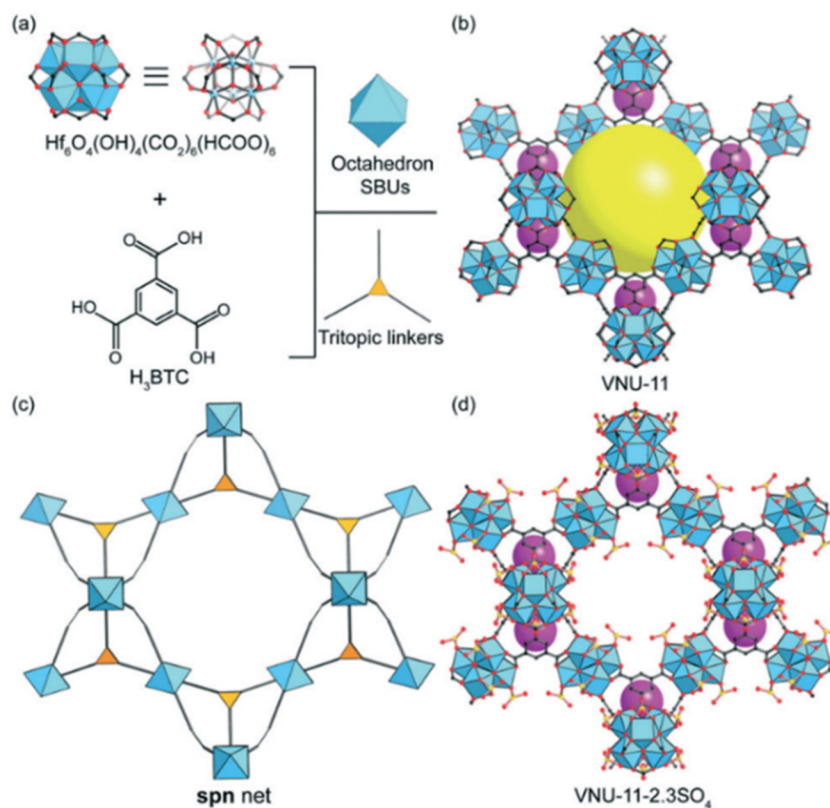


Fig. 4 Assembly of metal building units and organic linkers (a) forms the three-dimensional MOF, called VNU-11 (b), which features two distinct pores. The spn net (c) is shown for the MOF and its sulfate-functionalized structure (d). The spheres represent the cages. Reproduced with permission.<sup>119</sup> Reproduced from ref. 119 with permission from The Royal Society of Chemistry, copyright 2017.

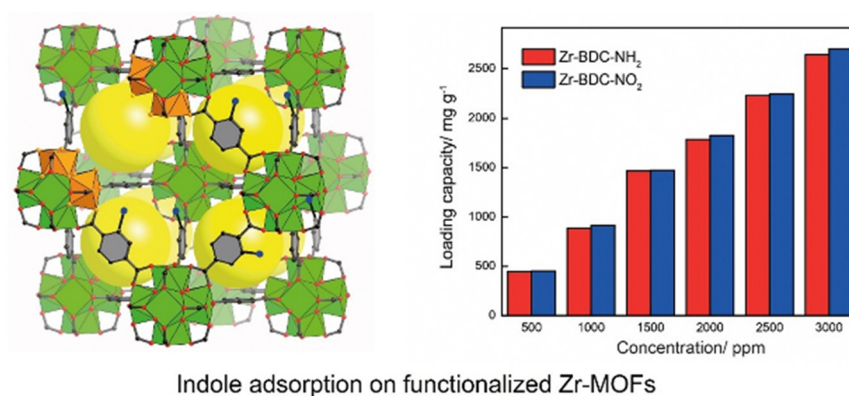


Fig. 5 The adsorption of indole on functionalized Zr-MOFs. The top left diagram: The porous structure of Zr-MOF, emphasizing its capacity to accommodate indole molecules. The bar chart on the top right: The indole loading capacities of amino-functionalized (Zr-BDC-NH<sub>2</sub>) and nitro-functionalized (Zr-BDC-NO<sub>2</sub>) MOFs across various concentrations, showing a consistent increase in adsorption with higher indole concentrations and slight performance differences between the two functional groups. The bottom panels: molecular-level visualization of the adsorption process, highlighting the interactions and distribution of indole within the framework pores, demonstrating the critical role of functional groups in optimizing adsorption efficiency. Reproduced with permission.<sup>123</sup> Reproduced from ref. 123 with permission from Elsevier, copyright 2017.

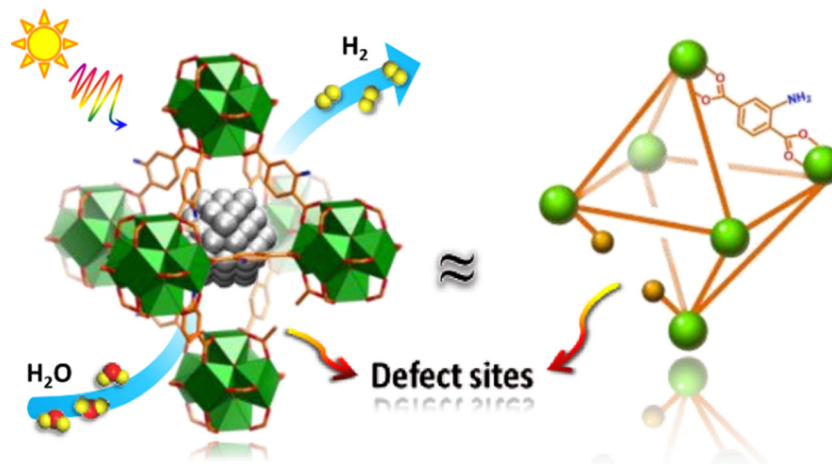


Fig. 6 The photocatalytic water splitting mechanism using a defect-engineered Zr-based MOF. The left diagram: The role of defect sites in the MOF structure, which enhance light absorption and facilitate the separation of water molecules ( $\text{H}_2\text{O}$ ) into hydrogen gas ( $\text{H}_2$ ) under sunlight irradiation. The right schematic: The atomic-level configuration of the defect sites, showcasing their contribution to the improved catalytic activity and hydrogen production efficiency.<sup>128</sup> Reproduced from ref. 128 with permission from Wiley, copyright 2019.

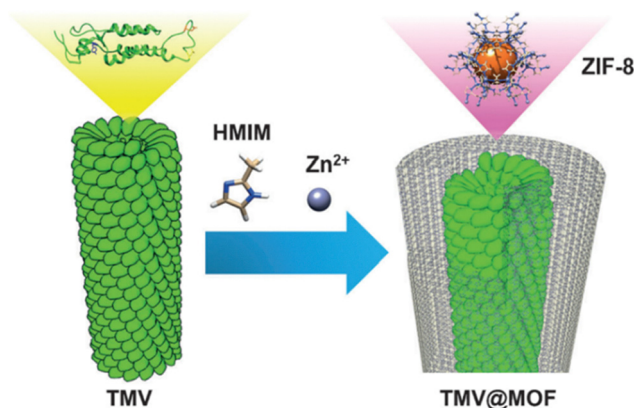


Fig. 7 The synthesis of a composite material combining TMV with ZIF-8. The process involves using TMV as a biological template, where  $\text{Zn}^{2+}$  ions and 2-methylimidazole (HMIM) coordinate to form the ZIF-8 shell around the TMV core. The resulting TMV@MOF structure integrates the biological features of TMV with the porous and protective properties of ZIF-8, offering potential applications in catalysis, biosensing, and drug delivery. Reproduced from ref. 132 with permission from Wiley, copyright 2016.

effective platforms for chemosensors for fluorine ion detection (Fig. 8).<sup>133</sup>

Owing to the fascinating nature and properties of MOFs, they are widely used in different applications such as storage and conversion applications,<sup>45</sup> water oxidation,<sup>48</sup> electrocatalysis,<sup>17,97</sup> solar energy,<sup>135</sup> photocatalysts,<sup>136</sup> and bio applications.<sup>137</sup> However, the main focus of this review paper is application of MOFs in gas sensing devices and so in the next parts we have delved more into this application.

#### 4. Toxic gases and resistive gas sensors

Air pollution is a significant issue in most countries which is caused by the rapid growth of different industries, transport

sections, mineral extraction, and more. Air pollution results from the existence of toxic gases, heavy metals, and particulate matter (PM) in the air. The main toxic gases in the air are  $\text{CO}$ ,  $\text{NO}_x$ ,  $\text{SO}_2$ ,  $\text{O}_3$ , and volatile organic compounds (VOCs).<sup>138,139</sup> On the other hand, other toxic gases (*e.g.*,  $\text{NH}_3$  and  $\text{H}_2\text{S}$ ), explosive gases (*e.g.*,  $\text{H}_2$  and  $\text{CH}_4$ ), and greenhouse gases (*e.g.*,  $\text{CO}_2$ ) may also exist in the surrounding environment, agricultural areas, and mines.<sup>140</sup> It is well known that air pollution has significant adverse effects on human health.<sup>141</sup> Specifically, it may cause cough, headache, asthma, cardiovascular diseases, diabetes, and high rates of hospitalization. In addition, air pollution can negatively affect early human life *via* cardiovascular, respiratory, mental, and other perinatal disorders and increase infant mortality.<sup>142,143</sup> Furthermore, air pollution was reported to cause cognitive dysfunction and the development of neurodegenerative phenomena underlying both Alzheimer's and Parkinson's disease.<sup>144</sup> Besides, it tends to affect happiness and life satisfaction.<sup>145</sup> Today, most people breathe polluted air with high concentrations of pollutants,<sup>146</sup> and more than 4.2 million premature deaths have been attributed to air pollution in 2016 alone.<sup>147</sup>

The olfactory system is very sensitive and complex (Fig. 9). It comprises receptor cells with  $\sim 900$  olfactory receptor genes.<sup>148</sup> On the other hand, with such a complex system, many toxic gases are only sensible at high concentrations. In addition, some gases are odorless, colorless, and tasteless, making them undetectable. Some diseases, such as Alzheimer's disease, can lead to olfactory dysfunction.<sup>149</sup>

Standardized techniques for gas monitoring, such as gas and ion chromatography, enable high sensitivity to trace amounts of gases. Unfortunately, they tend to be complicated, expensive, bulky, and off-line.<sup>150</sup> A sensor is a sensitive device that generates an electrical signal from a physical or chemical input stimulus. Gas sensors are chemical sensors where a specific property, such as electrical resistance, optical properties, or capacitance, changes upon exposure to target gases.<sup>151</sup>

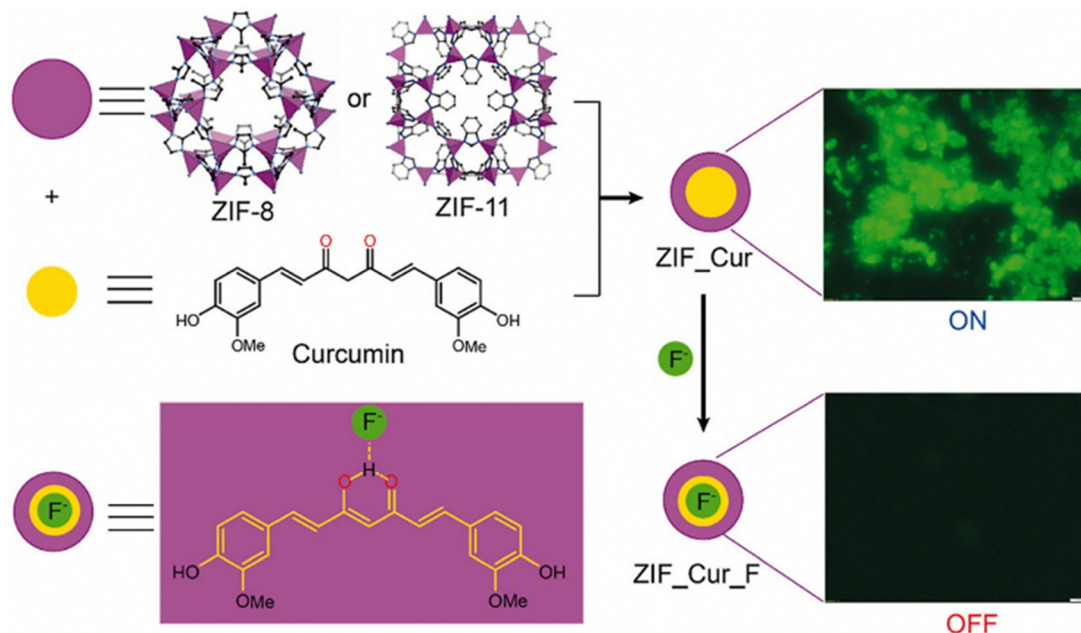


Fig. 8 ZIF-8 and ZIF-11 as effective platforms of curcumin-based on/off fluorescent chemosensors for fluorine ion detection. Reproduced from ref. 129 with permission from Elsevier, copyright 2021.

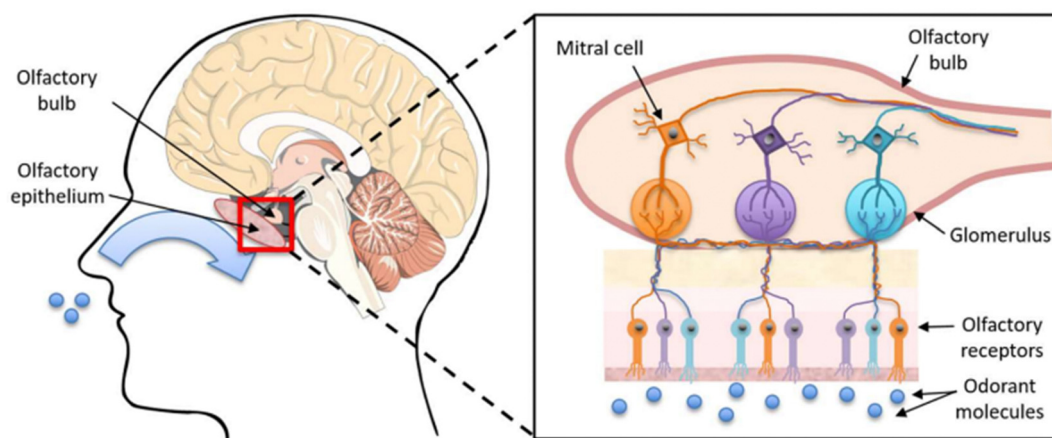


Fig. 9 Schematic illustration of the human olfactory system.<sup>149</sup> Reproduced from ref. 149 with permission from MDPI, copyright 2018.

Gas sensors come in various types, including catalytic,<sup>152</sup> gasochromic,<sup>153</sup> optical,<sup>154</sup> electrochemical,<sup>155</sup> capacitive,<sup>156,157</sup> transistor-type,<sup>158</sup> mass sensitive,<sup>159</sup> and resistive.<sup>160</sup> Resistive gas sensors are the simplest and cheapest sensing devices. In addition, they are most widely applied for the detection of gases due to their simple operation, small size, real-time operability, fast dynamics, and high stability.<sup>33,161,162</sup> Resistive gas sensors are manufactured by depositing a sensing layer on insulating substrates, like  $\text{Al}_2\text{O}_3$ , equipped with interdigitated electrodes and micro-heated at the back of the substrate (Fig. 10(a)–(c)).<sup>163</sup>

These gas sensors are primarily constructed using semiconductor metal oxides such as  $\text{SnO}_2$ <sup>164</sup> and  $\text{ZnO}$ .<sup>165</sup> However, despite their many advantages, they have significant limitations, such as high sensing temperatures, humidity interference, and poor selectivity.<sup>166</sup> Therefore, novel sensing materials or a

combination of novel and traditional sensing materials are needed to develop improved resistive sensors with superior capabilities such as better selectivity. MOFs, with their porous structures, provide highly specific surface areas (SSAs) and abundant functional sites like unsaturated metal sites, which are favorable for selective binding and sensing of gases. Accordingly, they are promising gas-sensing materials<sup>167</sup> for resistive gas sensors as well as for quartz crystal microbalances,<sup>168</sup> capacitive,<sup>169</sup> and other gas sensors. The following sections discuss MOF-based resistive gas sensors.

#### 4.1. MOFs as resistive gas sensors: an introduction

MOFs with unique features, such as very high SSA, abundant porosity, exceptional adsorption affinity, and outstanding surface chemistry, are promising materials for gas sensors,<sup>170–172</sup>

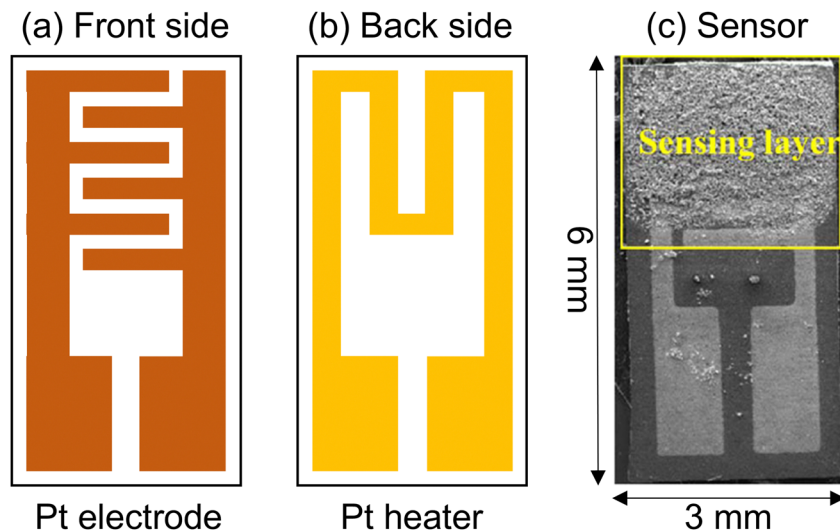


Fig. 10 Schematic of the (a) front side and (b) backside of a resistive gas sensor and (c) optical photograph of the final sensor.

supercapacitors, batteries, water purification, and catalysts.<sup>173</sup> For gas-sensing applications, their excellent tunability and chemical selectivity make them ideal for selective sensors.<sup>174</sup> One of the mechanisms contributing to their selectivity is molecular sieving, where smaller molecules can be adsorbed through the MOF apertures, while larger molecules are excluded and cannot pass through.<sup>174–176</sup> Furthermore, they can be used as a template to synthesize metal oxides, where the final product after annealing features a morphology and structure similar to that of the parent MOF, porous and with a high SSA.<sup>177–179</sup>

More specifically, MOF-based gas sensors offer several advantages for sensing applications: (i) the highly porous MOFs provide a large specific surface area (SSA) and numerous gas adsorption sites. Additionally, they contain unsaturated metal sites and functional groups that enhance gas adsorption. (ii) The porosity, geometry, and physicochemical features of MOFs can be tailored to improve selectivity for targeting gases.<sup>179</sup> In particular, in MOF-based gas sensors, achieving high selectivity often involves tailoring the material's properties to preferentially adsorb or interact with a desired gas, which can lead to a trade-off in which the sensitivity to other gases is reduced. In this regard, by altering the pore size structure or surface chemistry of a MOF, the selectivity to a particular gas may be enhanced, while its sensitivity to other gases may be decreased. For example, H<sub>2</sub> gas has a small kinetic diameter; by tailoring the pore size of the MOF in the range comparable with the kinetic diameter of H<sub>2</sub> gas, the resultant MOF gas sensor can not only show high response to H<sub>2</sub> gas, but at the same time can also show reduced response to other gases, leading to enhanced selectivity to H<sub>2</sub> gas.<sup>180,181</sup>

In resistive MOFs, resistance changes occur because of the adsorption of and interaction with the target gas. Furthermore, the redox reactions between gases and active metal sites in MOFs modulate the resistance. Moreover, the resistance of MOFs is influenced by structural changes resulting from gas adsorption. However, the limited electrical conductivity of most MOFs and their relatively low chemical stability impede their

application in pristine form.<sup>182,183</sup> In fact, MOFs often show poor conductivity because the metal cations in MOFs cannot migrate, and inert organic ligands attached to metal cations do not facilitate good electron flow.<sup>184,185</sup>

#### 4.2. MOF-based resistive gas sensors

**4.2.1. Pristine MOF gas sensors.** One of the features of MOF-based gas sensors is their good selectivity, which can be tuned *via* delicate control over their structure, porosity, chemical composition, and annealing temperature. Hence, Cu-MOFs were produced through a hydrothermal route at 120 °C/24 h. They were then annealed at 250 and 400 °C, labeled as Cu-MOF-250 and Cu-MOF-400, respectively. Based on thermal studies, the samples are stable at up to 250 °C in air. On the other hand, at higher temperatures, they decompose, and Cu oxidation occurs. At 250 °C, the Cu-MOF-400 sensor exhibited a stronger response to acetone (~2.5 to 40 ppm acetone) than the Cu-MOF-250 sensor. In addition, at 40 °C, it exhibited a stronger response to NO<sub>2</sub> (1.35 to 2 ppm) compared to the interfering gases. Therefore, the selectivity could be easily tuned by changing the sensing temperature.<sup>186</sup>

Nguyen *et al.* synthesized a novel Fe-MOF or VNU-15 with a high SSA (735 m<sup>2</sup> g<sup>-1</sup>) and a pore size of 10 Å to detect acetone (Fig. 11(a)).<sup>27</sup> At 50 °C, it exhibited a response of 1.7 to 10 ppm acetone (Fig. 11(b)–(d)). Based on the gas chromatography analysis, the appearance of CO<sub>2</sub> peaks upon exposure to acetone confirmed the oxidation of acetone at the sensing temperature. Acetone oxidation was facilitated at 50 °C by metal cations in VNU-15. In addition, Fe<sup>2+</sup>/Fe<sup>3+</sup> ions acted as catalytic sites to generate oxygen species, which accelerated the oxidation of -CH<sub>3</sub> in acetone. Because the formation energy of acetone (366 kJ mol<sup>-1</sup>) was lower than that of CO, C<sub>6</sub>H<sub>6</sub>, and C<sub>7</sub>H<sub>8</sub> gases (all > 370 kJ mol<sup>-1</sup>), it was readily dissociated at the sensor surface and generated a higher signal than other gases.

In another study, Co-MOF-I and II were prepared for H<sub>2</sub> gas sensing with a very high SSA of 2100 and 2420 m<sup>2</sup> g<sup>-1</sup>, respectively.

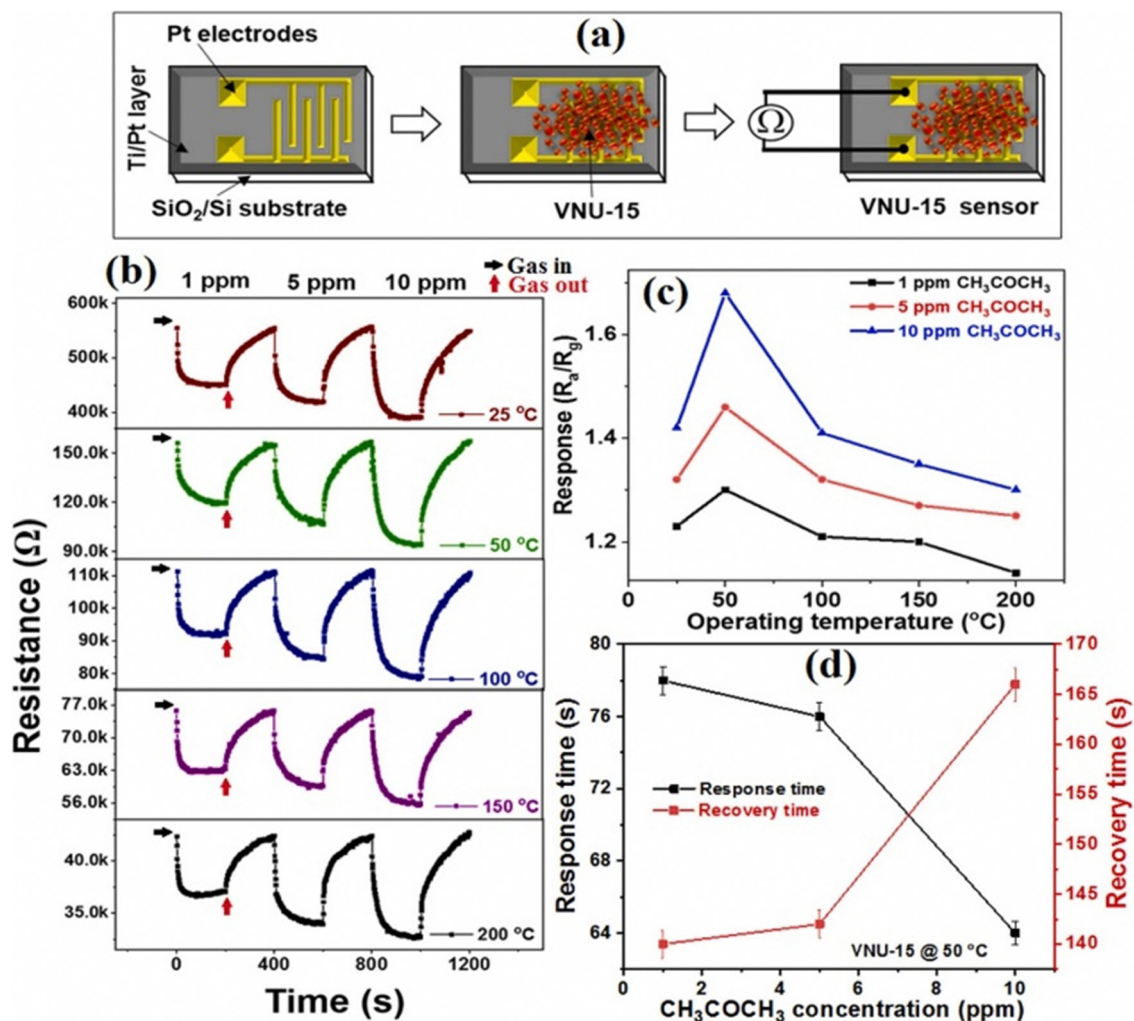


Fig. 11 (a) Schematic of the VNU-15 sensor. (b) Dynamic sensing graphs to acetone at various temperatures. (c) Response vs. temperature. (d) Response and recovery times to various concentrations of acetone at 50 °C.<sup>27</sup> Reproduced from ref. 27 with permission from Elsevier, copyright 2023.

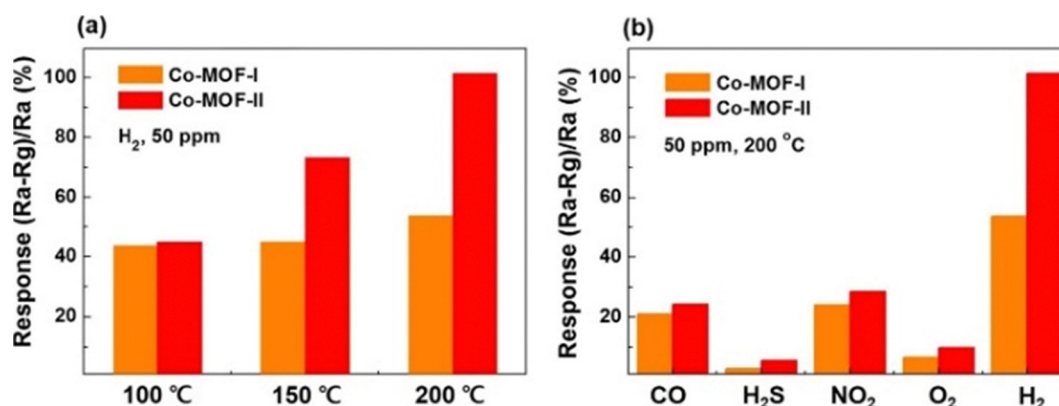


Fig. 12 (a) Comparison of the H<sub>2</sub> gas responses of Co-MOF-I and II sensors. (b) Selectivity histograms of Co-MOF-I and II sensors at 200 °C.<sup>16</sup> Reproduced from ref. 16 with permission from Elsevier, copyright 2020.

The response of the Co-MOF-II sensor was higher than that of the other sensor at all temperatures (Fig. 12(a)). In addition, it exhibited higher selectivity to CO than to the interfering gases (Fig. 12(b)).

In addition to a higher SSA, the Co-MOF-II sensor featured a larger pore volume (1.27 cm<sup>3</sup> g<sup>-1</sup>) and smaller pore size (23.2 Å) than the other sensor (1.10 cm<sup>3</sup> g<sup>-1</sup> and 27.6 Å, respectively). In particular,

smaller pores led to easier interaction between the open Co sites and small H<sub>2</sub> molecules. Moreover, the size of H<sub>2</sub> gas molecules was smaller than that of other gases, which led to a better response and selectivity to H<sub>2</sub> gas. Furthermore, the excellent response was related to the higher Co(II)/Co concentration in the sensor, where the higher amount of the open Co sites in the Co-MOF-II sensor increased the probability of attaching the H<sub>2</sub> molecules at the sensor surface.<sup>16</sup>

CO is a particularly hazardous gas because it is also colorless, odorless, and tasteless. Inhalation of CO primarily affects the cardiovascular and nervous systems.<sup>187</sup> When CO enters the body, it attaches to hemoglobin (Hb), generating COHb that considerably decreases the oxygen-carrying ability of blood. Hence, death is likely even upon exposure to relatively small amounts of CO gas.<sup>188</sup> To address this problem, Ni-MOFs (Ni-VNU-74-I and II) were synthesized for CO sensing. At 200 °C, the Ni-VNU-74-II sensor showed a response of ~1.65 to CO gas (50 ppm) (Fig. 13(a)–(d)). The better performance is mainly due to a higher SSA (2350 m<sup>2</sup> g<sup>-1</sup>) and smaller pore size (23.6 Å) of the Ni-VNU-74-II sensor compared to the other sensor (2020 m<sup>2</sup> g<sup>-1</sup> and 27.3 Å). The interaction between CO and Ni<sup>2+</sup> ions resulted in the effective adsorption of CO at the sensor surface. In addition, FTIR spectroscopy revealed signals at ~2200 and 2085 cm<sup>-1</sup>, which were assigned to the Ni<sup>2+</sup>-CO bonds and the sub-carbonyls of Ni,

respectively. These findings confirm the strong interaction between CO gas and Ni<sup>2+</sup> ions.<sup>29</sup>

#### 4.2.2. MOF composite-based gas sensors

**4.2.2.1. MOF/carbon-based composite gas sensors.** Due to the low conductivity of MOFs, composites with materials of higher conductivity, such as graphene, conducting polymers (CPs), and metal oxides, are used to enhance MOF performance.<sup>189</sup> Graphene, which consists of a single layer of carbon atoms arranged in a nanosheet-like morphology, is one such material. It has a high SSA, high stability, mechanical flexibility, and high conductivity owing to the high carrier mobility and low electrical noise.<sup>190,191</sup> However, it has no bandgap and is hydrophobic, which makes it challenging to use for gas sensing. Reduced graphene oxide (rGO) has many defects, high conductivity, and high hydrophilicity, and it can be used in place of graphene for sensing studies.<sup>192,193</sup> Therefore, a combination of rGO with high conductivity and MOFs can enhance the sensing properties of the resulting nanocomposite. In one study, the NiO-MOF and NiO-MOF/rGO nanocomposites were hydrothermally prepared at 120 °C. The SSA of NiO-MOF was 810 m<sup>2</sup> g<sup>-1</sup>, and it increased to 872 m<sup>2</sup> g<sup>-1</sup> after incorporating rGO due to the 2D morphology and high SSA of rGO. The composite sensor responded more strongly to CO than to NH<sub>3</sub> and SO<sub>2</sub> gases. In addition, the response was higher than that of the pristine NiO-MOF sensor—mainly because of a higher

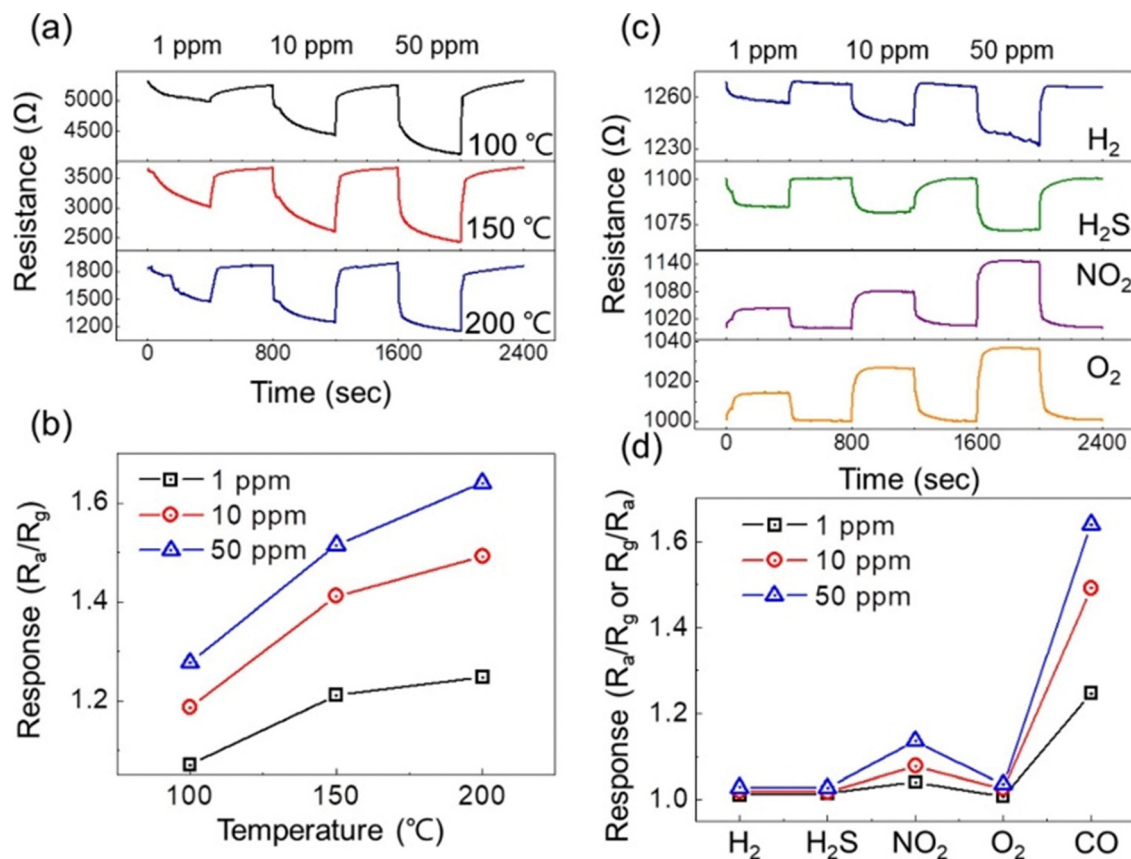


Fig. 13 (a) Sensing graphs of the Ni-MOF sensor to CO gas at various temperatures. (b) Response vs. temperature. (c) Sensing graphs of the Ni-MOF sensor to different gases at 200 °C. (d) Response to different gases at 200 °C.<sup>29</sup> Reproduced from ref. 29 with permission from Elsevier, copyright 2020.

SSA and the formation of Ni-MOF/rGO heterojunctions. The comparable kinetic diameter of CO to the aperture size of NiO-MOF, the high conductivity of rGO, the porous nature of Ni-MOF, and the formation of Ni-MOF/rGO heterojunctions all contribute to the enhanced sensing capabilities.<sup>194</sup> Another study developed a flexible Cu(INA)<sub>2</sub>/rGO composite for NH<sub>3</sub> gas sensing at room temperature, using a combination of MOF and reduced graphene oxide. NH<sub>3</sub> gas readily diffused into and adsorbed on Cu(INA)<sub>2</sub> due to the porous nature of the sensing material. In addition, the sensor's high SSA provided adsorption sites for NH<sub>3</sub> gas. The adsorption ability of Cu(INA)<sub>2</sub> and the high conductance of rGO improved the response to NH<sub>3</sub> gas.<sup>195</sup>

In another study involving MOF composites with graphene derivatives, a graphene acid (GA)/UiO-66-NH<sub>2</sub> composite was synthesized by covalently bonding GA with the UiO-66-NH<sub>2</sub> MOF through amide bonds. With the hierarchical pores, the composite showed a high SSA of 598 m<sup>2</sup> g<sup>-1</sup>, a pore volume of 1.09 cm<sup>3</sup> g<sup>-1</sup>, and good conductivity because of the presence of GA and good stability. Both GA and UiO-66-NH<sub>2</sub> sensors showed low responses to CO<sub>2</sub> gas. Although pristine GA is very conductive due to delocalized  $\pi$ -electrons, it did not have any favorable sites for CO<sub>2</sub> adsorption. Pristine UiO-66-NH<sub>2</sub>, however, has sufficient interaction sites for CO<sub>2</sub> gas adsorption, but its resistance is very high. However, the GA/UiO-66-NH<sub>2</sub> composite offered a good and rapid response to CO<sub>2</sub> gas at 200 °C due to synergistic effects between the two materials. Raman analysis indicates that CO<sub>2</sub> only weakly interacts with CO-NH above 200 °C. In composite sensors, the MOF controlled the space between the GA layers and led to the creation of adsorption sites at the functional groups at the GA-MOF interface.<sup>196</sup>

An interesting application of gas sensors is the monitoring of the freshness of fruit,<sup>197</sup> where the emission of certain gases is used as an indicator of fruit quality.<sup>198</sup> On the other hand, for these applications, flexible gas sensors, which retain their performance upon stretching, tilting, and bending,<sup>199</sup> are preferred over rigid sensors because they can be easily attached to fruit skin. Ethylene is a hormone that facilitates the growth and maturation of plants. It is released during the growth and decay of fruit. Generally, fruit rapidly ripens and decays because of the autocatalytic action of the accumulated ethylene.<sup>200,201</sup> For these reasons, an ethylene sensor was fabricated to detect fruit freshness and spoilage of kiwi that uses a single-walled carbon nanotube (SWCNT)/Pd NPs/Cu-MOF-74 (SPM) nanocomposite. The nanocomposite was prepared using a self-assembly technique. Flexibility was achieved by depositing the sensor onto a flexible PET substrate. The SSA (13 m<sup>2</sup> g<sup>-1</sup>) of the SWCNTs increased to 92 m<sup>2</sup> g<sup>-1</sup> for the composite sensor. In other words, the composite sensor provided many adsorption sites for ethylene gas. Moreover, the water contact angle (WCA) of the SPM composite was 34.87°, significantly higher than that of Cu-MOF-74 (24.30°), which confirms the effectiveness of SWCNTs in enhancing the hydrophobicity of the sensor. In addition, the SPM sensor was highly resistant to humidity above 40–70%. The sensor exhibited a response of 34.2% to 100 ppb C<sub>2</sub>H<sub>4</sub>. C<sub>2</sub>H<sub>4</sub> was easily oxidized on Pd NPs because of

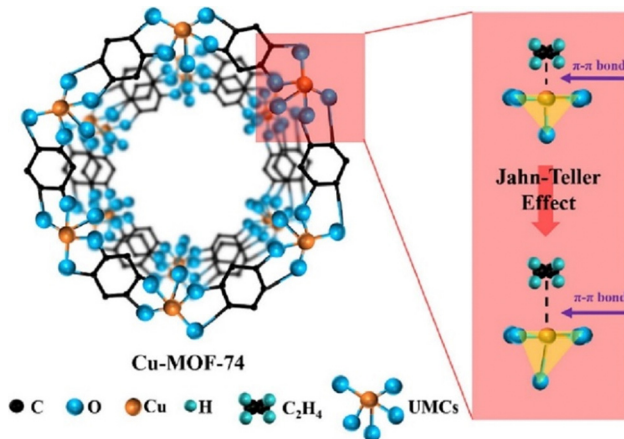


Fig. 14 Schematic illustration of the Cu-MOF-74 structure showing Jahn–Teller distortion.<sup>202</sup> Reproduced from ref. 202 with permission from Elsevier, copyright 2024.

the catalytic effect of Pd. The released electrons migrated to the sensor surface, which decreased resistance. Cu-MOF-74 contained Cu<sup>2+</sup> ions, which formed a covalent bond with C<sub>2</sub>H<sub>4</sub> *via*  $\pi$ – $\pi$  stacking interactions. In addition, the bonds between Cu-MOF-74 and C<sub>2</sub>H<sub>4</sub> expanded, and the MOF was distorted into a stable pseudo-octahedral shape because of the Jahn–Teller effect (Fig. 14).

The sensor performance to monitor the ripeness and decomposition of kiwi was assessed by attaching the sensor to a kiwi at room temperature and 75% relative humidity (Fig. 15a). The sensor generated various signals that could be related to the ripeness and decomposition of kiwi (Fig. 15(a)–(c)).<sup>202</sup>

SO<sub>2</sub> is a significant factor in air pollution, which can adversely affect human health and lead to respiratory issues and mortality.<sup>203</sup> Hence, flexible SO<sub>2</sub> gas sensors were manufactured based on Ni-MOF/OH-SWCNTs and Ni-MOF/OH-MWCNTs. The sensor with SWCNTs performed better for SO<sub>2</sub> gas and could detect 0.5 ppm SO<sub>2</sub>. The sensing signal was attributed to a high SSA, good conductivity, and the formation of heterojunctions between Ni-MOF and SWCNTs.<sup>204</sup>

**4.2.2.2. MOF/CP-based composite gas sensors.** Conducting polymers (CPs) have electrical conductivity, and therefore, can be used for sensing applications. Polyaniline (PANI) is a CP with unusually high electrical conductance,<sup>205</sup> and like rGO, it can be composited with MOFs to further increase the electrical conductivity and the overall sensing performance of the MOF-PANI composite.<sup>206</sup> Hence, a composite sensor consisting of SiO<sub>2</sub>-coated Cu-MOF, graphene and PANI was prepared. Cu-MOF and graphene in the composite were connected *via* PANI. The sensor showed a high SSA of 760 m<sup>2</sup> g<sup>-1</sup> and a micropore volume of 0.35 cm<sup>3</sup> g<sup>-1</sup>. In other words, it could offer a high SSA to gas molecules. The NH<sub>3</sub> gas could diffuse into the deeper regions of the sensor because of the many pores in the sensing material. As a result, NH<sub>3</sub> gas was detected at levels as low as 0.6 ppm with relatively fast dynamics. The enhanced response to NH<sub>3</sub> gas was due to the high sensitivity of PANI to NH<sub>3</sub>, PANI

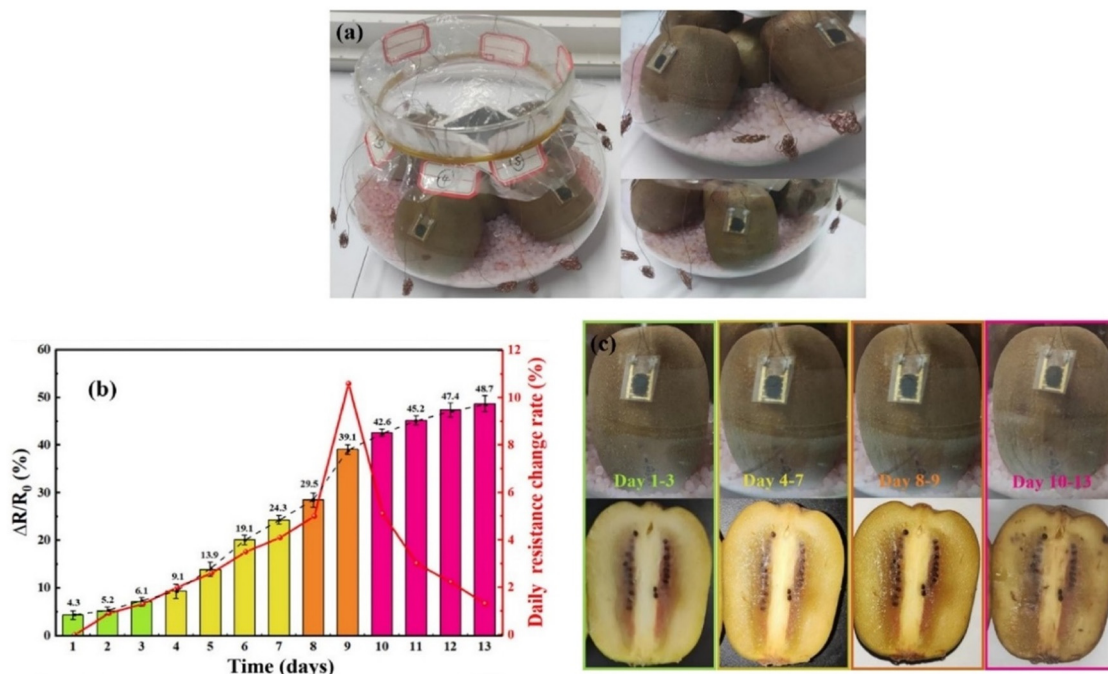


Fig. 15 (a) Flexible sensors attached to a kiwi fruit. (b) Response and change in resistance of the sensor during 13 days. (c) Optical images of the kiwi after various time intervals.<sup>202</sup> Reproduced from ref. 202 with permission from Elsevier, copyright 2024.

donates one proton to  $\text{NH}_3$ , forming  $\text{NH}_4^+$  ions, which increase the sensor resistance. In addition, significant resistance modulation occurred because of the creation of heterojunctions between Cu-MOF/PANI and rGO, which contributes to the sensing signal.<sup>207</sup>

Like most MOFs, the UiO-66- $\text{NH}_2$  MOF has high resistance, which hinders its usage in sensing studies and hence conductive polymers such as poly(3,4-ethylenedioxythiophene):poly(styrene sulfonate) (PEDOT:PSS), which features high conductivity,<sup>208</sup> can be added to address this problem. Therefore, a UiO-66- $\text{NH}_2$ /PEDOT:PSS composite was synthesized for toluene sensing using a hydrothermal reaction. It exhibited a response of 1.42 to toluene (10 ppm) at room temperature. Operation at room temperature can significantly lower the energy consumption of the sensing device.

However, the response time of the sensor was long (340 s) due to low kinetics at room temperature. Furthermore, the high SSA of the UiO-66- $\text{NH}_2$  MOF and the conductivity of the PEDOT:PSS polymer affected the output of the sensor. Moreover, at the contact areas, electrons migrated from PEDOT:PSS to UiO-66- $\text{NH}_2$  to equilibrate the Fermi levels, which resulted in the generation of potential barriers. In the presence of toluene, electrons were released to the sensor surface through a reaction with chemisorbed oxygen species, which lowered both the potential barrier height and electrical resistance.<sup>209</sup>

In another study on CP/MOF composite sensors, a  $\text{Cu}_3(\text{HHTP})_2$  MOF/PVA composite mixed with an ionic liquid (IL) was synthesized to enhance conductivity for  $\text{H}_2\text{S}$  sensing. The composite was hydrophilic due to the presence of  $-\text{OH}$  groups in each ionic liquid molecule. In an acidic  $\text{H}_2\text{S}$  gas

atmosphere, the molecules of  $\text{H}_2\text{S}$  reacted with oxygen ions on the PVA, ionic liquid, and Cu-MOF, which led to the release of electrons. Hence, a flow of charged ions and protons became possible. In addition, the highly conjugated linker also improved the conductivity of the composite sensor. Moreover, Cu-MOF had 1.55 nm pores, which exceeded the size of the  $\text{H}_2\text{S}$  molecule (0.36 nm). Therefore,  $\text{H}_2\text{S}$  gas easily diffused within the MOF, resulting in high sensitivity and selectivity to this gas.<sup>210</sup>

A composite gas sensor using MOF-5 microparticles/chitosan (CS) was fabricated for  $\text{H}_2\text{S}$  gas sensing, and a glycerol ionic liquid was added to enhance the conductivity of the sensor. MOF-5 nanoparticles dispersed within the CS-IL matrix enhanced the transport of  $\text{H}_2\text{S}$  through the membrane because of the porosity of MOF-5. The sensor exhibited a 91% response to  $\text{H}_2\text{S}$  gas (100 ppm) in just 8 seconds. The enhanced capability was attributed to the high SSA and the porous MOF, along with the excellent conductivity of the sensor as a result of the CS-IL matrix.<sup>210</sup>

**4.2.2.3. MOF/metal oxide-based composite gas sensors.** ZIFs are MOFs with a 3D mesh structure consisting of tetrahedral  $\text{MN}_4$  ( $\text{M}$  = metal cation) and tetrahedral clusters, which are connected *via* imidazolate linkers with high porosity and a high internal SSA. Both ZIF-8 and ZIF-71 are widely used for sensing applications. These materials have pore sizes of 3.4 Å and 4.8 Å, respectively. Accordingly, ZIF-8 is typically used to detect small molecules, such as  $\text{H}_2$ , while ZIF-71 is employed to sense large molecules, such as ethanol.<sup>211</sup> Drobeck *et al.*<sup>180</sup> coated ZnO nanowires (NWs) with a thin layer of ZIF-8 using a

hydrothermal route at 100 °C/24 hours for selective H<sub>2</sub> sensing. At 300 °C, the ZIF-8-coated sensor showed a stronger response to H<sub>2</sub> gas than to C<sub>7</sub>H<sub>8</sub> and C<sub>6</sub>H<sub>6</sub> gases because of its molecular sieving effect. In fact, these gases were unable to pass this layer and reach the ZnO surface because the average pore size of ZIF-8 (3.4 Å) was below that of C<sub>7</sub>H<sub>8</sub> (5.92 Å) and C<sub>6</sub>H<sub>6</sub> (5.27 Å) gases.

On the other hand, H<sub>2</sub> gas with a smaller molecular size (2.89 Å) than the aperture size of ZIF-8 easily diffused through and reached the surface of ZnO. The response of the ZIF-8 coated sensor was slightly lower than that of the pristine ZnO because of the presence of ZIF-8 (with lower conductivity) and the prevention of adsorption of all H<sub>2</sub> gas molecules on the ZnO NWs. In other words, ZIF-based gas sensors can be tuned to respond to a specific gas.

Since the stability of MOFs is generally low, a composite of MOFs with metal oxides may increase the overall stability of the resulting sensor and increase the gas-sensitive output. For this reason, an In<sub>2</sub>O<sub>3</sub>@MIL-68(In) composite was synthesized hydrothermally at 80, 100, and 120 °C (Fig. 16). A sensor prepared hydrothermally at 100 °C showed a response of 18 to 100 ppm HCHO gas, which was six times higher than that of pristine In<sub>2</sub>O<sub>3</sub>. The excellent formaldehyde sensing performance was attributed to the low bond-dissociation energy. The bond energy of formaldehyde is 368 kJ mol<sup>-1</sup>, whereas the bond energies of ethanol, methanol, methane, and acetone are all higher than 400 kJ mol<sup>-1</sup>. Therefore, formaldehyde decomposed quickly at the sensing temperature and released more electrons than other gases. Furthermore, the sea urchin shape morphology and the presence of MIL-68(In) on In<sub>2</sub>O<sub>3</sub> enhanced the sensor's response.<sup>212</sup> The detection of formaldehyde is essential as exposure to it can cause allergies,

asthma, pulmonary damage, and cancer from contaminated foods, water, and air.<sup>213</sup>

NO<sub>2</sub> is a hazardous gas emitted mainly from the combustion of fossil fuels. Exposure to this gas causes coughing and respiratory problems, such as asthma.<sup>214</sup> In addition, the intensity of a COVID-19 infection is increased in the presence of NO<sub>2</sub> gas.<sup>207,215</sup> Shin *et al.*<sup>216</sup> coated a titanium-based MOF on SnO<sub>2</sub> NWs to enable the selective detection of NO<sub>2</sub>. In a dry atmosphere at 200 °C, the responses of the pristine and Ti-MOF-coated SnO<sub>2</sub> sensors to 2 ppm NO<sub>2</sub> were 5.4 and 4.3, respectively. Under humid conditions, however, the response of the coated sensor was higher (Fig. 17(a)–(d)). The water contact angles (WCAs) of the pristine and Ti-MOF-coated sensors were 10° and 123°, respectively (Fig. 17(e)), indicating the hydrophobicity of the Ti-MOF coating, which is highly beneficial for gas-sensing in a humid atmosphere.

#### 4.2.3. Functionalized MOF composite-based gas sensors.

H<sub>2</sub> is highly explosive in air (4–75 vol%) and has a low ignition energy as well as a high flame propagation rate.<sup>217,218</sup> On the other hand, it is very small and can easily diffuse and leak through storage containers.<sup>219</sup> A novel amine-functionalized Zn-BDC-NH<sub>2</sub> MOF was synthesized hydrothermally for H<sub>2</sub> gas sensing. It had a high SSA of 890 m<sup>2</sup> g<sup>-1</sup> with a pore size of ~13 Å. At 50 °C, it showed a response to 3 to 10 ppm H<sub>2</sub>. Fig. 18(a)–(c) shows a scheme of the sensing mechanism, where the width of the EDL decreases in the H<sub>2</sub> gas atmosphere. The high SSA and high porosity offer many gas-adsorption sites.

The presence of open metal sites of Zn provided additional adsorption sites for H<sub>2</sub> gas. H<sub>2</sub> gas with a small molecular size of 0.289 nm could quickly diffuse into all regions of the sensing layer, which resulted in better sensor response to H<sub>2</sub> relative to interfering gases. The functionalization of –NH<sub>2</sub> enhanced the

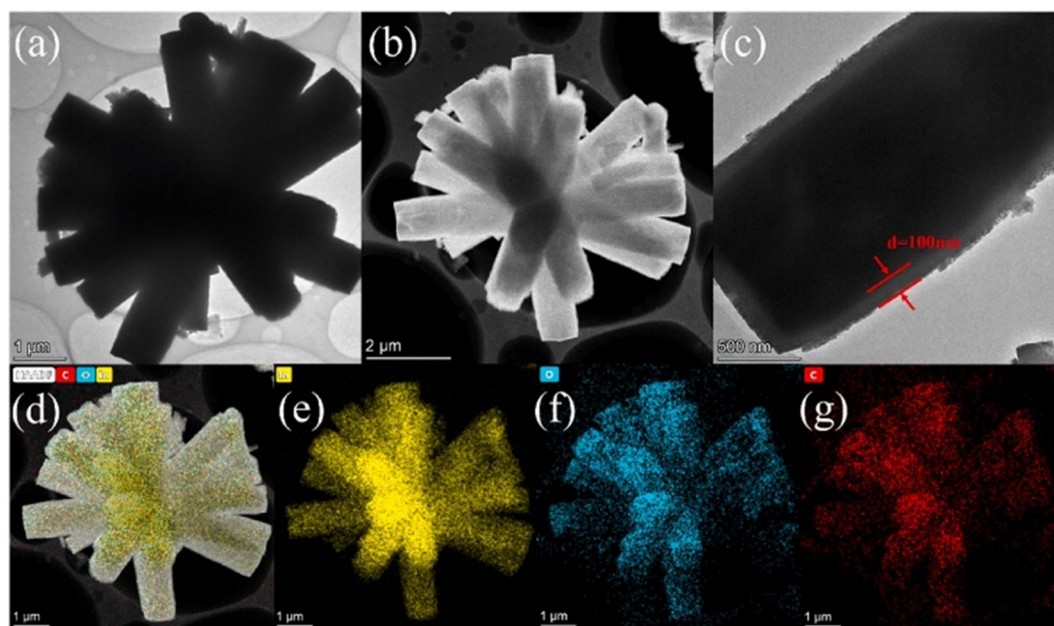


Fig. 16 (a) and (b) TEM and (c) HRTEM views of In<sub>2</sub>O<sub>3</sub>@MIL-68(In) prepared at 100 °C under hydrothermal conditions. (d)–(g) TEM-EDS elemental mapping analysis.<sup>212</sup> Reproduced from ref. 212 with permission from Elsevier, copyright 2023.

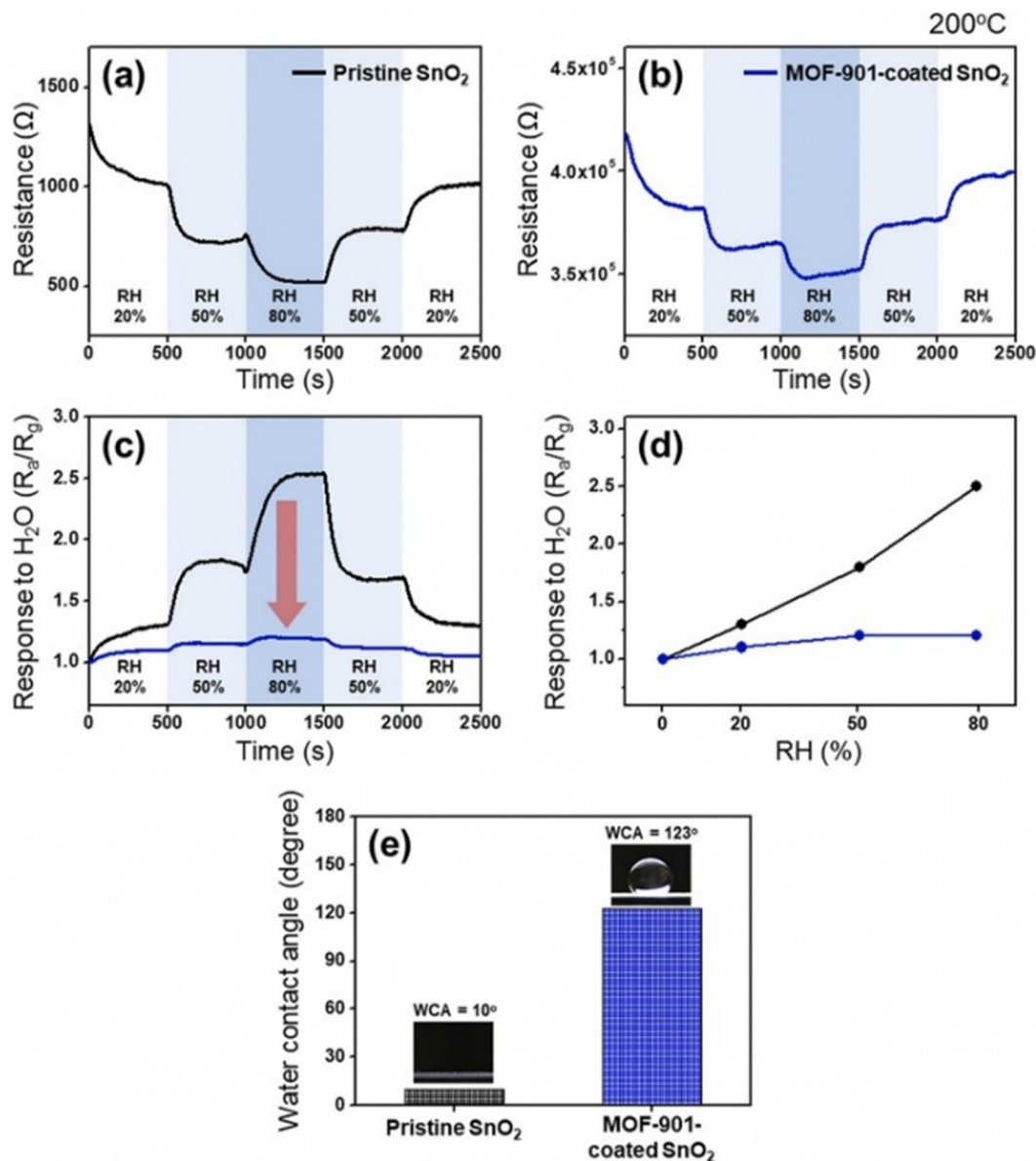


Fig. 17 Dynamic sensing curves of (a) pristine SnO<sub>2</sub> NW and (b) Ti-MOF-coated SnO<sub>2</sub> NW sensors to various levels of RH. (c) Comparison of dynamic sensing responses to various levels of RH. (d) Corresponding calibration graphs. (e) WCA values of the gas sensors.<sup>216</sup> Reproduced from ref. 216 with permission from Elsevier, copyright 2023.

number of active sites for H<sub>2</sub>, which improved the adsorption capability of H<sub>2</sub>.

Moreover, the reaction of H<sub>2</sub> gas with Zn<sub>4</sub>O(CO<sub>2</sub>)<sub>6</sub> helped to decrease the sensor resistance. H<sub>2</sub> gas was chemisorbed at the “Zn” and “O” sites. Upon adsorption on “O” sites, O–H bonds were formed through strong hybridization between the H-s and O-p orbitals. Moreover, the delocalization of electrons between the Zn and O–H bonds facilitated the surface metallization of Zn, with a significant change in conductance.<sup>220</sup>

Few studies have explored the incorporation of noble metals on MOFs for gas sensing. In this context, sulfone-functionalized Zr-MOF (Zr-BPDC-SO<sub>2</sub>) and Pd-loaded Zr-BPDC-SO<sub>2</sub> composites were hydrothermally prepared at 120 °C/24 hours. Zr-BPDC-SO<sub>2</sub> exhibited a stronger response to ethanol,

while Pd/Zr-BPDC-SO<sub>2</sub> showed better sensing with respect to H<sub>2</sub> gas. At 150 °C, the Zr-BPDC-SO<sub>2</sub> gas sensor manifested a response of 1.45 to 100 ppm ethanol. Also, the response of the Pd/Zr-BPDC-SO<sub>2</sub> sensor was ~2 to 10 ppm H<sub>2</sub> gas at 150 °C. The SSAs of the two sensors were 1360 and 530 m<sup>2</sup> g<sup>-1</sup>, respectively. In addition, the pore sizes of Zr-BPDC-SO<sub>2</sub> and Pd/Zr-BPDC-SO<sub>2</sub> were 12 and 6 Å, respectively. Therefore, following Pd-loading, some pores were closed, which caused a decrease in both SSA and pore size and a lower response to ethanol compared to the Zr-BPDC-SO<sub>2</sub> sensor. Fig. 19(a) and (b) show the reaction of the Zr-BPDC-SO<sub>2</sub> and Pd/Zr-BPDC-SO<sub>2</sub> gas sensors to ethanol and H<sub>2</sub> gases, respectively. Furthermore, Fig. 19(c) shows the variation of the hole accumulation layer (HAL) of gas sensors in air, ethanol, and H<sub>2</sub> gas. In terms of H<sub>2</sub>

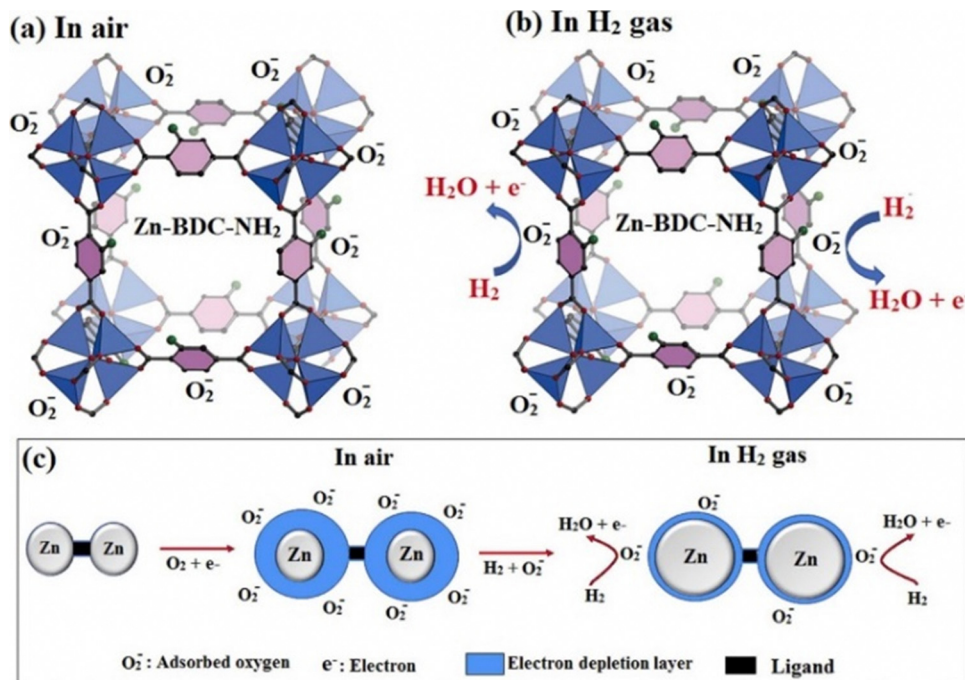


Fig. 18 Schematic illustration of the  $\text{H}_2$  gas sensing mechanism of Zn-BDC-NH<sub>2</sub> in (a) air and (b)  $\text{H}_2$  atmospheres, and (c) change of the thickness of the EDL of Zn-BDC-NH<sub>2</sub> in air and  $\text{H}_2$  atmospheres.<sup>220</sup> Reproduced from ref. 220 with permission from Elsevier, copyright 2022.

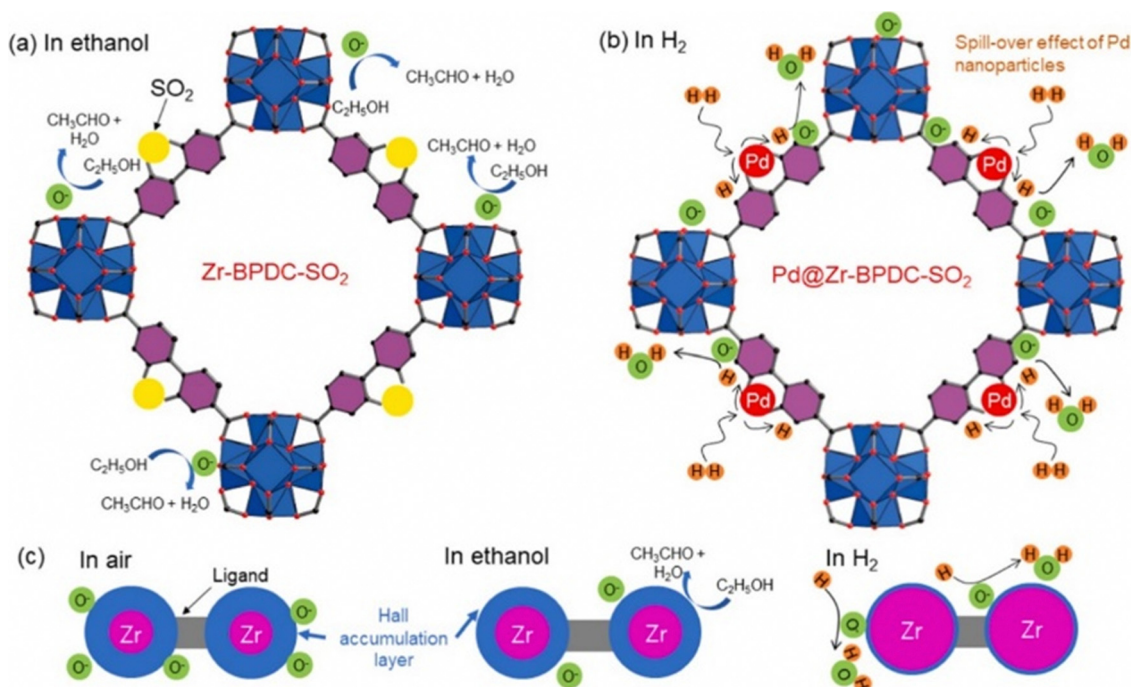
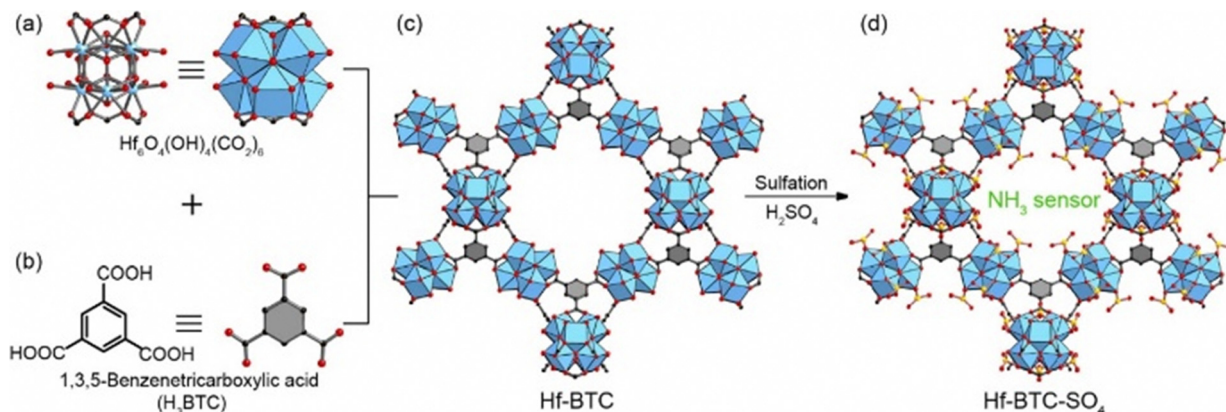


Fig. 19 Schematic illustrating the gas sensing mechanism of (a) Zr-BPDC-SO<sub>2</sub> and (b) Pd/Zr-BPDC-SO<sub>2</sub> gas sensors to ethanol and  $\text{H}_2$ , respectively. (c) Modulation of HAL in air, ethanol, and  $\text{H}_2$  atmospheres.<sup>130</sup> Reproduced from ref. 130 with permission from Elsevier, copyright 2021.

gas sensing, the catalytic effect of Pd plays an important role. First,  $\text{H}_2$  gas molecules adsorb easily on Pd and dissociate into atomic species. Under the spillover effect, they move to the neighboring sensing material and then readily react with adsorbed oxygen. Thus, a strong response to  $\text{H}_2$  gas was observed. In addition, PdH<sub>x</sub>,

formed in an  $\text{H}_2$  gas atmosphere, exhibits different resistance compared to metallic Pd due to Pd's ability to adsorb  $\text{H}_2$  gas, which substantially modulates its resistance.<sup>130</sup>

$\text{NH}_3$  is a hazardous and corrosive gas that can irritate the eyes, nose, and lungs and damage the immune system.<sup>221</sup>



**Fig. 20** Schematic illustration of the synthesis and functionalization of Hf-BTC. (a) The  $\text{Hf}_6\text{O}_4(\text{OH})_4(\text{CO}_2)_{12}$  cluster as the secondary building unit (SBU). (b) 1,3,5-Benzenetricarboxylic acid ( $\text{H}_3\text{BTC}$ ) as the organic linker. (c) Formation of the Hf-BTC MOF *via* coordination between Hf clusters and BTC linkers. (d) Sulfation of Hf-BTC using  $\text{H}_2\text{SO}_4$  to obtain Hf-BTC- $\text{SO}_4$  for ammonia ( $\text{NH}_3$ ) sensor.<sup>222</sup> Reproduced from ref. 222 with permission from Elsevier, copyright 2022.

In air, it produces aerosols that exhibit a temperature-reducing effect and negatively affect the global greenhouse balance.<sup>222</sup> Moreover, it is considered a medical biomarker for kidney disorders.<sup>223</sup> An Hf-BTC MOF was synthesized and functionalized *via* the  $\text{SO}_4$  group to boost the sensing response to  $\text{NH}_3$  (Fig. 20).

The Hf-BTC MOF showed a very high SSA of  $1100 \text{ m}^2 \text{ g}^{-1}$  and an average pore size of  $15 \text{ \AA}$  that promoted sensing reactions through the rapid diffusion of gases. At  $100 \text{ }^\circ\text{C}$ , the sensor exhibited a response of 2.1 to 10 ppm  $\text{NH}_3$ . In addition to the high SSA, the excellent crystallinity of Hf-BTC- $\text{SO}_4$  allowed  $\text{NH}_3$  to be adsorbed on the sensor through strong host/guest interactions. The  $\text{SO}_4$  groups, which were Brønsted acid sites, interacted with the Lewis acid sites on the  $\text{Hf}_6$  cluster. This led to a strong interaction with  $\text{NH}_3$  and improved the response to  $\text{NH}_3$ . In addition, the good selectivity to  $\text{NH}_3$  was due to the interactions of N atoms in  $\text{NH}_3$  with metal sites on the MOF. The kinetic diameter of  $\text{NH}_3$  ( $0.26 \text{ nm}$ ) was also smaller than

that of other gases, which enabled easy penetration through the pores inside the sensing layer.<sup>222</sup>

Table 2 compares the gas sensing properties of various MOF-based gas sensors. The main criteria for comparing sensing performance are response, sensing temperature, selectivity, and response and recovery times. Obviously, lower sensing temperature is a beneficial factor for gas sensors as it leads to reduced power consumption. Also, higher sensing response is better for practical application. Selectivity to a particular gas is important for practical application to avoid the false alarms. Faster dynamics in terms of response and recovery times is also a beneficial factor for real applications. Specially, for highly toxic gases such as  $\text{NO}_2$  and  $\text{CO}$ , swift response time is highly important from a safety point of view. Overall, MOF-based gas sensors have been successfully used for the detection of various gases. The sensing temperature is often low, compared with metal oxide gas sensors. However, response and recovery times are usually longer than those of metal oxide-based gas sensors,

**Table 2** Comparison of gas sensing performance of various MOF-based gas sensors

Sensing material	Specific surface areas ( $\text{m}^2 \text{ g}^{-1}$ )	$T$ ( $^\circ\text{C}$ )	Gas	Conc. (ppm)	Response ( $R_a/R_g$ ) or ( $R_g/R_a$ ) or $[(\Delta R/R_a) \times 100]$	Response/recovery time (s/s)	Detection limit (ppm)	Ref.
Fe-MOF	735	50	Acetone	10	1.7	64/78	1	27
Co-MOF-II	2420	200	$\text{H}_2$	50	101.4%	—/—	1	16
Ni-VNU-74-II	2020	200	$\text{CO}$	50	1.65	—/—	1	29
NiO-MOF/rGO	872	25	$\text{CO}$	25	$\sim 0.9\%$	30/75	25	194
$\text{Cu}(\text{INA})_2/\text{rGO}$	Not mentioned	25	$\text{NH}_3$	50	$\sim 4.651\%$	—/—	50	195
$\text{GA}/\text{UiO}-66\text{-NH}_2$	598	200	$\text{CO}_2$	500 000	8.6%	18.5/18.7	—	196
SWCNT/Pd NPs/Cu-MOF-74	92	25	$\text{C}_2\text{H}_4$	0.1	34.2%	200/50	0.1	202
$\text{SiO}_2$ -coated Cu-MOF/graphene/PANI	756	25	$\text{NH}_3$	1	—	30/180	0.6	207
UiO-66- $\text{NH}_2$ MOF	876	25	$\text{C}_7\text{H}_8$	10	1.42	340/—	1	209
$\text{Cu}_3(\text{HHTP})_2$ MOF/PVA	279.997	25	$\text{H}_2\text{S}$	100	91%	8/—	1	210
ZIF-8 coated ZnO NWs	1760	300	$\text{H}_2$	50	1.44	—/—	10	180
$\text{In}_2\text{O}_3@/\text{MIL}-68$	133.48	300	HCHO	100	18	28/43	5	212
Ti-MOF-coated $\text{SnO}_2$ NWs	Not mentioned	200	$\text{NO}_2$	2	4.3	672/843	2	216
Zr-BPDC- $\text{SO}_2$	1360	150	$\text{C}_2\text{H}_5\text{OH}$	100	1.383	—/—	10	130
$\text{Pd}/\text{Zr-BPDC-}\text{SO}_2$	530	150	$\text{H}_2$	100	1.947	—/—	10	130
Hf-BTC- $\text{SO}_4$	1100	100	$\text{NH}_3$	10	2.1	72/138	1	222

mainly due to working at low temperatures. Also, generally detection limits are down to 1 ppm, which is higher than those of metal oxide gas sensors, which are generally in the ppb range. Also, by properly adjusting pore sizes and the use of different strategies such as functionalization, MOF gas sensors often can have better selectivity relative to metal oxide gas sensors.

## 5. Degradation and long-term stability of MOF gas sensors

Despite their numerous advantages, the practical deployment of MOFs is often limited by their stability and degradation under operational conditions. Generally, three types of degradation mechanisms have been identified for MOFs:

(i) Hydrolytic degradation: exposure to moisture can lead to the hydrolysis of metal–ligand bonds in MOFs, resulting in structural collapse. For instance, the  $Zr_6O_4(OH)_4$  secondary building unit in some MOFs undergoes significant changes in chemical and thermal stability upon incorporation of different organic linkers, affecting their resistance to hydrolysis.<sup>224</sup>

(ii) Thermal degradation: elevated temperatures can weaken the coordination bonds within MOFs, leading to decomposition. The thermal stability of a MOF is influenced by factors such as the strength of metal–ligand bonds and the robustness of its framework.<sup>225</sup>

(iii) Chemical degradation: exposure to acidic or basic environments can disrupt the coordination bonds in MOFs. For example, carboxylate-based MOFs with high-valent metal ions exhibit remarkable robustness in acidic water but show moderate resistance in alkaline environments. The degradation in basic solutions is attributed to the high affinity between hydroxide ions and high-valency metal ions.<sup>225</sup>

Also, factors influencing the long-term stability of MOFs are as follows:<sup>225</sup>

(i) Framework hydrophobicity: hydrophobic frameworks can repel water molecules, reducing the likelihood of hydrolytic degradation. This property is particularly beneficial for MOFs intended for application in humid or aqueous environments.

(ii) Metal–ligand bond strength: stronger coordination bonds between metal ions and ligands enhance the resilience of MOFs to environmental stressors. Hence, MOFs constructed with inert metal ions and robust, hydrophobic linkers demonstrate increased resistance to hydrolysis.

In the case of MOFs for gas sensing applications, the main stability issues are related to temperature and humidity. In particular, low thermal stability at the sensing temperature causes changes in the phase and composition of the MOF sensor, affecting the overall sensing performance. In this regard, some strategies such as chemical treatment after synthesis to increase the strength of the framework, composite formation and the use of appropriate ligands can increase the stability of MOFs. Integrating MOFs with other materials with high thermal stability can enhance their mechanical strength and thermal stability. Also, applying protective coatings to MOFs can shield them from

moisture, contaminants, and other environmental factors that may cause degradation. Advances in MOF coatings have led to the development of composites that exhibit improved stability and functionality. These coatings not only protect the MOF structures but also enhance their applicability in various fields, including gas sensing.<sup>226,227</sup>

Also, humid air generally has a negative effect on the performance of almost all MOFs. In fact, in humid air, water molecules are adsorbed on the surface of MOFs, decreasing the number of adsorption sites and leading to a decrease of sensing response. However, the use of hydrophobic MOFs can somewhat overcome this negative humidity effect.<sup>216</sup> Contaminants can occupy or block the MOF pores, resulting in a decrease of the effective surface area and sensing performance.

## 6. Conclusion and outlooks

This study explored the synthesis methods for preparing MOFs and their applications as resistive gas sensors. MOFs were synthesized *via* different routes, including hydrothermal/solvothermal, microwave, ionothermal, pyrolysis, mechanochemical, electrochemical, and template-directed synthesis methods. Scalability and industrial feasibility remain key challenges for MOF-based sensors due to high synthesis costs, complex fabrication, and energy-intensive processes. To address these issues, alternative synthesis methods such as mechanochemical, microwave-assisted, and electrochemical approaches have been explored for faster and more cost-effective production. Additionally, integrating MOFs with scalable substrates and developing continuous-flow synthesis methods can enhance their industrial applicability. Furthermore, the functionalization of MOFs is a crucial factor that enhances their versatility and tailors their properties for specific applications. The functionalization of MOFs was achieved through several strategies, including post-synthetic modification, incorporation of functional linkers, metal site functionalization, coordinative unsaturation, encapsulation of functional molecules, and surface functionalization. Highly porous MOFs with a high SSA are promising materials for gas-sensing applications. In addition, with tuneable pore sizes, they can act as molecular sieves for the selective detection of target gases. However they generally show low conductivity, which limits their application in pristine form.

Because stability is a critical factor in gas sensors, both chemical and physical durability play a significant role in maintaining performance over extended use. Chemically, the incorporation of stable metal clusters (*e.g.*, Zr-, Ti-, and Hf-based MOFs) enhances resistance to hydrolysis and oxidation, while the addition of carbon materials and conductive polymers as well as doping with metal or redox-active species to facilitate charge transport improves moisture resistance and electrical conductivity, reducing framework degradation. Physically, these composites exhibit superior structural integrity compared to pristine MOFs, as carbon materials help prevent framework collapse during repeated gas adsorption/desorption

cycles, and polymer matrices enhance mechanical robustness and adhesion to substrates.

Different materials with higher conductivity than MOFs, like carbon materials, metal oxides, and conductive polymers, were added to MOFs to increase the overall conductance and sensing performance of the resulting composite. Also, in the composite form, MOFs can act as molecular sieves, preventing the adsorption of undesired gases or humidity on the surface of the sensing layer. For example, coating metal oxides with MOFs can reduce the interference caused by humidity and enhance the selectivity of the sensor.

We also explained the gas sensing performance of various MOF-based gas sensors, demonstrating the fact that MOFs have high potential to be used as gas sensing devices. However, to further boost their performance, they can be integrated with metal oxides, metal sulfides, and MXenes. In particular, MXenes with high conductivity, tunable properties, and high surface area are the most promising materials to be integrated with MOFs to significantly increase the sensing performance at low temperatures. With high potential of working at low temperatures down to room temperature along with relatively good flexibility, MOFs can be used for the realization of flexible/wearable gas sensing devices. However, when sensing temperature is high, by use of different strategies such as UV illumination or operation of the sensor in self-heating mode the sensing temperature and power consumption can be significantly decreased. Operation in self-heating mode means applying an external voltage directly to the sensor electrodes, which induces heat internally within the sensing material *via* the Joule heating effect.

## Author contributions

Linh Ho Thuy Nguyen: conceptualization; writing – review & editing. Ali Mirzaei: conceptualization; writing – review & editing. Jin-Young Kim: writing – review & editing. Thang Bach Phan: writing – review & editing. Lam Dai Tran: writing – review & editing. Kevin C.-W. Wu: writing – review & editing. Hyoun Woo Kim: supervision. Sang Sub Kim: review & supervision. Tan Hoang Le Doan: writing – review & editing; supervision.

## Data availability

We would like to confirm that no primary research results, software or code have been included and no new data were generated or analysed as part of this review.

## Conflicts of interest

There are no conflicts to declare.

## Acknowledgements

This study was supported by the Vietnam National University, Ho Chi Minh City, under grant number TX2025-50-01. In addition,

this research was supported by the Nano & Material Technology Development Program through the National Research Foundation of Korea (NRF), funded by the Ministry of Science and ICT (RS-2024-00412249).

## References

- 1 H. Furukawa, K. E. Cordova, M. O’Keeffe and O. M. Yaghi, The Chemistry and Applications of Metal-Organic Frameworks, *Science*, 2013, **341**(6149), 1230444.
- 2 H. Wang, X. Dong, J. Lin, S. J. Teat, S. Jensen, J. Cure, E. V. Alexandrov, Q. Xia, K. Tan, Q. Wang, D. H. Olson, D. M. Proserpio, Y. J. Chabal, T. Thonhauser, J. Sun, Y. Han and J. Li, Topologically guided tuning of Zr-MOF pore structures for highly selective separation of C6 alkane isomers, *Nat. Commun.*, 2018, **9**(1), 1745.
- 3 Y. Yao, X. Zhao, G. Chang, X. Yang and B. Chen, Hierarchically Porous Metal–Organic Frameworks: Synthetic Strategies and Applications, *Small Struct.*, 2023, **4**(1), 2200187.
- 4 G. Lin, B. Zeng, J. Li, Z. Wang, S. Wang, T. Hu and L. Zhang, A systematic review of metal organic frameworks materials for heavy metal removal: Synthesis, applications and mechanism, *Chem. Eng. J.*, 2023, **460**, 141710.
- 5 N. H. Ly, N. B. Nguyen, H. N. Tran, T. T. H. Hoang, S.-W. Joo, Y. Vasseghian, H. Kamyab, S. Chelliapan and J. J. Klemeš, Metal-organic framework nanopesticide carrier for accurate pesticide delivery and decrement of groundwater pollution, *J. Cleaner Prod.*, 2023, **402**, 136809.
- 6 Y. Ye, Y. Xie, Y. Shi, L. Gong, J. Phipps, A. M. Al-Enizi, A. Nafady, B. Chen and S. Ma, A Microporous Metal–Organic Framework with Unique Aromatic Pore Surfaces for High Performance C2H6/C2H4 Separation, *Angew. Chem., Int. Ed.*, 2023, **62**(21), e202302564.
- 7 Z. Zhu, H. Tsai, S. T. Parker, J.-H. Lee, Y. Yabuuchi, H. Z. H. Jiang, Y. Wang, S. Xiong, A. C. Forse, B. Dinakar, A. Huang, C. Dun, P. J. Milner, A. Smith, P. Guimarães Martins, K. R. Meihaus, J. J. Urban, J. A. Reimer, J. B. Neaton and J. R. Long, High-Capacity, Cooperative CO2 Capture in a Diamine-Appended Metal–Organic Framework through a Combined Chemisorptive and Physisorptive Mechanism, *J. Am. Chem. Soc.*, 2024, **146**(9), 6072–6083.
- 8 B. Jie, H. Lin, Y. Zhai, J. Ye, D. Zhang, Y. Xie, X. Zhang and Y. Yang, Mechanism, design and application of fluorescent recognition based on metal organic frameworks in pollutant detection, *Chem. Eng. J.*, 2023, **454**, 139931.
- 9 Z. Xu, Z. Wu, S. Huang, K. Ye, Y. Jiang, J. Liu, J. Liu, X. Lu and B. Li, A metal-organic framework-based immunomodulatory nanoplatform for anti-atherosclerosis treatment, *J. Controlled Release*, 2023, **354**, 615–625.
- 10 B. Q. G. Le and T. L. H. Doan, Trend in biodegradable porous nanomaterials for anticancer drug delivery, *Wiley Interdiscip. Rev.: Nanomed. Nanobiotechnol.*, 2023, **15**(4), e1874.

- 11 H. Hu and Y. Wang, Recent advances in metal–organic frameworks as emerging platforms for immunoassays, *TrAC, Trends Anal. Chem.*, 2024, **171**, 117520.
- 12 M. H. Teplensky, M. Fantham, P. Li, T. C. Wang, J. P. Mehta, L. J. Young, P. Z. Moghadam, J. T. Hupp, O. K. Farha, C. F. Kaminski and D. Fairen-Jimenez, Temperature Treatment of Highly Porous Zirconium-Containing Metal–Organic Frameworks Extends Drug Delivery Release, *J. Am. Chem. Soc.*, 2017, **139**(22), 7522–7532.
- 13 Y. Shi, Z. Wang, Z. Li, H. Wang, D. Xiong, J. Qiu, X. Tian, G. Feng and J. Wang, Anchoring LiCl in the Nanopores of Metal–Organic Frameworks for Ultra-High Uptake and Selective Separation of Ammonia, *Angew. Chem., Int. Ed.*, 2022, **61**(47), e202212032.
- 14 J. Wang, J. Liu, H. Wang, M. Zhou, G. Ke, L. Zhang, J. Wu, Z. Gao and D. Lu, A comprehensive transformer-based approach for high-accuracy gas adsorption predictions in metal-organic frameworks, *Nat. Commun.*, 2024, **15**(1), 1904.
- 15 A. R. Yuvaraj, A. Jayarama, D. Sharma, S. S. Nagarkar, S. P. Duttagupta and R. Pinto, Role of metal-organic framework in hydrogen gas storage: A critical review, *Int. J. Hydrogen Energy*, 2024, **59**, 1434–1458.
- 16 D.-K. Nguyen, J.-H. Lee, T. L.-H. Doan, T.-B. Nguyen, S. Park, S. S. Kim and B. T. Phan, H<sub>2</sub> gas sensing of Co-incorporated metal-organic frameworks, *Appl. Surf. Sci.*, 2020, **523**, 146487.
- 17 K.-K. Liu, Z. Meng, Y. Fang and H.-L. Jiang, Conductive MOFs for electrocatalysis and electrochemical sensor, *eScience*, 2023, **3**(6), 100133.
- 18 H. Li, K. Wang, Y. Sun, C. T. Lollar, J. Li and H.-C. Zhou, Recent advances in gas storage and separation using metal–organic frameworks, *Mater. Today*, 2018, **21**(2), 108–121.
- 19 M.-H. D. Dang, T. T. T. Nguyen, B. Q. G. Le, L. H. T. Nguyen, N. X. D. Mai, M. V. Nguyen, P. H. Tran and T. L. H. Doan, An effective combination of reusable Pd@MOF catalyst and deep eutectic solvents for high-performance C–C coupling reaction, *J. Ind. Eng. Chem.*, 2022, **111**, 111–120.
- 20 L. H. T. Nguyen, T. T. T. Nguyen, P. H. Tran, Y. Kawazoe, H. M. Le and T. L. H. Doan, Zr and Hf-metal-organic frameworks: Efficient and recyclable heterogeneous catalysts for the synthesis of 2-arylbenzoxazole via ring open pathway acylation reaction, *J. Catal.*, 2019, **374**, 110–117.
- 21 Y. Wang, W. Chen, J. Fu and Y. Liu, Efficient air water harvesting of TpPa-1 COFs@LiCl composite driven by solar energy, *eScience*, 2023, **3**(4), 100154.
- 22 S. Bazzazan, K. Moeinabadi-Bidgoli, Z. A. Lalami, S. Bazzazan, M. Mehrarya, F. E. Yeganeh, F. Hejabi, I. Akbarzadeh, H. Noorbazargan, M. Jahanbakhshi, N. Hosseinkhannazer and E. Mostafavi, Engineered UIO-66 metal-organic framework for delivery of curcumin against breast cancer cells: An in vitro evaluation, *J. Drug Delivery Sci. Technol.*, 2023, **79**, 104009.
- 23 M. Pourmadadi, S. Ostovar, M. M. Eshaghi, M. Rajabzadeh-Khosroshahi, S. Safakhah, S. Ghotekar, A. Rahdar and A. M. Díez-Pascual, Nanoscale metallic-organic frameworks as an advanced tool for medical applications: Challenges and recent progress, *Appl. Organomet. Chem.*, 2023, **37**(3), e6982.
- 24 L. H. T. Nguyen, Y. Thi Dang, T. T. T. Nguyen, B. Q. G. Le, N. X. D. Mai, H. V. Nguyen, M.-T. Le, T. B. Phan and T. L. H. Doan, Pore engineering of biomolecule-based metal–organic framework nanocarriers for improving loading and release of paclitaxel, *New J. Chem.*, 2022, **46**(14), 6630–6635.
- 25 S. Wei, R. Hou, Q. Zhu, I. Shakir, Z. Fang, X. Duan and Y. Xu, Hybrid materials based on covalent organic frameworks for photocatalysis, *InfoMat*, 2025, e12646.
- 26 J. Zhao, Z. Chen, S. Liu, P. Li, S. Yu, D. Ling and F. Li, Nano-bio interactions between 2D nanomaterials and mononuclear phagocyte system cells, *BMEMat*, 2024, **2**(2), e12066.
- 27 L. H. Thuy Nguyen, S. T. Navale, D. H. Yang, H. T. T. Nguyen, T. B. Phan, J.-Y. Kim, A. Mirzaei, T. L. H. Doan, S. S. Kim and H. W. Kim, Fe-based metal-organic framework as a chemiresistive sensor for low-temperature monitoring of acetone gas, *Sens. Actuators, B*, 2023, **388**, 133799.
- 28 M. Zhan, C. Ge, S. Hussain, A. S. Alkorbi, R. Alsaiani, N. A. Alhemiary, G. Qiao and G. Liu, Enhanced NO<sub>2</sub> gas-sensing performance by core-shell SnO<sub>2</sub>/ZIF-8 nanospheres, *Chemosphere*, 2022, **291**, 132842.
- 29 D.-K. Nguyen, J.-H. Lee, T.-B. Nguyen, T. Le Hoang Doan, B. T. Phan, A. Mirzaei, H. W. Kim and S. S. Kim, Realization of selective CO detection by Ni-incorporated metal-organic frameworks, *Sens. Actuators, B*, 2020, **315**, 128110.
- 30 J. Abdi, N. M. Mahmoodi, M. Vossoughi and I. Alemzadeh, Synthesis of magnetic metal-organic framework nanocomposite (ZIF-8@SiO<sub>2</sub>@MnFe<sub>2</sub>O<sub>4</sub>) as a novel adsorbent for selective dye removal from multicomponent systems, *Microporous Mesoporous Mater.*, 2019, **273**, 177–188.
- 31 A. K. Singh, N. Jaiswal, R. K. Gautam and I. Tiwari, Development of g-C<sub>3</sub>N<sub>4</sub>/Cu-DTO MOF nanocomposite based electrochemical sensor towards sensitive determination of an endocrine disruptor BPSIP, *J. Electroanal. Chem.*, 2021, **887**, 115170.
- 32 Z. Xiao, L. B. Kong, S. Ruan, X. Li, S. Yu, X. Li, Y. Jiang, Z. Yao, S. Ye, C. Wang, T. Zhang, K. Zhou and S. Li, Recent development in nanocarbon materials for gas sensor applications, *Sens. Actuators, B*, 2018, **274**, 235–267.
- 33 M.-S. Yao, W.-H. Li and G. Xu, Metal–organic frameworks and their derivatives for electrically-transduced gas sensors, *Coord. Chem. Rev.*, 2021, **426**, 213479.
- 34 N. Garg, A. Deep and A. L. Sharma, Metal-organic frameworks based nanostructure platforms for chemo-resistive sensing of gases, *Coord. Chem. Rev.*, 2021, **445**, 214073.
- 35 F. Dai, X. Cui, Y. Luo, D. Zhang, N. Li, Y. Huang and Y. Peng, Ultrathin MOF nanosheet-based resistive sensors for highly sensitive detection of methanol, *Chem. Commun.*, 2022, **58**(82), 11543–11546.
- 36 I. Strauss, A. Mundstock, M. Treger, K. Lange, S. Hwang, C. Chmelik, P. Rusch, N. C. Bigall, T. Pichler, H. Shiozawa and J. Caro, Metal–Organic Framework Co-MOF-74-Based

- Host–Guest Composites for Resistive Gas Sensing, *ACS Appl. Mater. Interfaces*, 2019, **11**(15), 14175–14181.
- 37 X. Shi, Y. Shan, M. Du and H. Pang, Synthesis and application of metal-organic framework films, *Coord. Chem. Rev.*, 2021, **444**, 214060.
- 38 X. Zhang, J. Wang, X.-X. Dong and Y.-K. Lv, Functionalized metal-organic frameworks for photocatalytic degradation of organic pollutants in environment, *Chemosphere*, 2020, **242**, 125144.
- 39 V. Bon, I. Senkovska, M. S. Weiss and S. Kaskel, Tailoring of network dimensionality and porosity adjustment in Zr- and Hf-based MOFs, *CrystEngComm*, 2013, **15**(45), 9572–9577.
- 40 T. L. H. Doan, H. L. Nguyen, H. Q. Pham, N.-N. Pham-Tran, T. N. Le and K. E. Cordova, Tailoring the Optical Absorption of Water-Stable ZrIV- and HfIV-Based Metal–Organic Framework Photocatalysts, *Chem. – Asian J.*, 2015, **10**(12), 2660–2668.
- 41 W. Lu, Z. Wei, Z.-Y. Gu, T.-F. Liu, J. Park, J. Park, J. Tian, M. Zhang, Q. Zhang, T. Gentle III, M. Bosch and H.-C. Zhou, Tuning the structure and function of metal–organic frameworks via linker design, *Chem. Soc. Rev.*, 2014, **43**(16), 5561–5593.
- 42 C. McKinstry, R. J. Cathcart, E. J. Cussen, A. J. Fletcher, S. V. Patwardhan and J. Sefcik, Scalable continuous solvothermal synthesis of metal organic framework (MOF-5) crystals, *Chem. Eng. J.*, 2016, **285**, 718–725.
- 43 A. A. Bhoite, K. V. Patil, R. S. Redekar, P. S. Patil, V. A. Sawant and N. L. Tarwal, Solvothermal synthesis of binder free Ni-MOF thin films for supercapacitor electrodes, *J. Solid State Chem.*, 2023, **326**, 124192.
- 44 Y. Ban, Y. Li, X. Liu, Y. Peng and W. Yang, Solvothermal synthesis of mixed-ligand metal–organic framework ZIF-78 with controllable size and morphology, *Microporous Mesoporous Mater.*, 2013, **173**, 29–36.
- 45 Z. Meng, Z. Qiu, Y. Shi, S. Wang, G. Zhang, Y. Pi and H. Pang, Micro/nano metal–organic frameworks meet energy chemistry: A review of materials synthesis and applications, *eScience*, 2023, **3**(2), 100092.
- 46 L. Huelsenbeck, H. Luo, P. Verma, J. Dane, R. Ho, E. Beyer, H. Hall, G. M. Geise and G. Giri, Generalized Approach for Rapid Aqueous MOF Synthesis by Controlling Solution pH, *Cryst. Growth Des.*, 2020, **20**(10), 6787–6795.
- 47 W. Xuan, R. Ramachandran, C. Zhao and F. Wang, Influence of synthesis temperature on cobalt metal-organic framework (Co-MOF) formation and its electrochemical performance towards supercapacitor electrodes, *J. Solid State Electrochem.*, 2018, **22**(12), 3873–3881.
- 48 M. Huang, C. Cao, L. Liu, W. Wei, Q.-L. Zhu and Z. Huang, Controlled synthesis of MOF-derived hollow and yolk–shell nanocages for improved water oxidation and selective ethylene glycol reformation, *eScience*, 2023, **3**(5), 100118.
- 49 I. Akpınar, X. Wang, K. Fahy, F. Sha, S. Yang, T. W. Kwon, P. J. Das, T. Islamoglu, O. K. Farha and J. F. Stoddart, Biomimetic Mineralization of Large Enzymes Utilizing a Stable Zirconium-Based Metal–Organic Frameworks, *J. Am. Chem. Soc.*, 2024, **146**(8), 5108–5117.
- 50 H. Wang, Y. Ren, X. Feng and H. Jiang, Ultrathin 2D Porphyrin-Based Zr-MOF Nanosheets as Heterogeneous Catalysts for Styrene Epoxidation and Benzylic C-H Oxidation, *ChemCatChem*, 2024, **16**(15), e202400119.
- 51 T. E. Webber, W.-G. Liu, S. P. Desai, C. C. Lu, D. G. Truhlar and R. L. Penn, Role of a Modulator in the Synthesis of Phase-Pure NU-1000, *ACS Appl. Mater. Interfaces*, 2017, **9**(45), 39342–39346.
- 52 T. T. Thu Nguyen, L. H. Thuy Nguyen, N. X. Dat Mai, H. K. Thi Ta, T. L. Thuong Nguyen, U.-C. Nguyen Le, B. T. Phan, N. N. Doan and T. Le Hoang Doan, Mild and Large-scale Synthesis of Nanoscale Metal–Organic Framework Used as a Potential Adenine-based Drug Nanocarrier, *J. Drug Delivery Sci. Technol.*, 2020, 102135.
- 53 W. Y. Siew, N. H. H. Abu Bakar, M. Abu Bakar and A. Zainal Abidin, Influence of various Cu/Fe ratios on the surface properties of green synthesized Cu-Fe-BTC and its relation to methylene blue adsorption, *J. Hazard. Mater.*, 2021, **416**, 125846.
- 54 R. K. A. Amali, H. N. Lim, I. Ibrahim, Z. Zainal and S. A. A. Ahmad, Energy-efficient green synthesis of metal-organic frameworks for effective electrochemical nitrite sensing, *Appl. Mater. Today*, 2023, **33**, 101871.
- 55 R. Udaya Rajesh, T. Mathew, H. Kumar, A. Singhal and L. Thomas, Metal-organic frameworks: Recent advances in synthesis strategies and applications, *Inorg. Chem. Commun.*, 2024, **162**, 112223.
- 56 F. Sun, H. Guo, W. Zhang, T. Li, X. Lu, L. Zhao, D. Zhou and Q. Xia, Catalytic epoxidation of limonene and air with high performance by zirconium cobalt bimetallic MOF lamellar materials, *Mol. Catal.*, 2024, **557**, 113958.
- 57 H. R. Abid, A. Hanif, A. Keshavarz, J. Shang and S. Iglauer, CO<sub>2</sub> and H<sub>2</sub> Adsorption Performance of the Metal–Organic Framework HKUST-1 by Modified Synthesis Strategies, *Energy Fuels*, 2023, **37**(10), 7260–7267.
- 58 Y. R. Rosyara, A. Muthurasu, K. Chhetri, I. Pathak, T. H. Ko, P. C. Lohani, D. Acharya, T. Kim, D. Lee and H. Y. Kim, Highly Porous Metal–Organic Framework Entrapped by Cobalt Telluride–Manganese Telluride as an Efficient Bifunctional Electrocatalyst, *ACS Appl. Mater. Interfaces*, 2024, **16**(8), 10238–10250.
- 59 Y. Xie, T. Zhang, B. Wang and W. Wang, The Application of Metal–Organic Frameworks in Water Treatment and Their Large-Scale Preparation: A Review, *Materials*, 2024, **17**(9), 1972.
- 60 D. Sud and G. Kaur, A comprehensive review on synthetic approaches for metal-organic frameworks: From traditional solvothermal to greener protocols, *Polyhedron*, 2021, **193**, 114897.
- 61 H. Wang, Y. Dai, Y. Wang and L. Yin, One-pot solvothermal synthesis of Cu–Fe-MOF for efficiently activating peroxy-monosulfate to degrade organic pollutants in water: Effect of electron shuttle, *Chemosphere*, 2024, **352**, 141333.
- 62 P. Kukkar, D. Kukkar, H. Sammi, K. Singh, M. Rawat, P. Singh, S. Basu and K.-H. Kim, A facile means for the improvement of sensing properties of metal-organic

- frameworks through control on the key synthesis variables, *Sens. Actuators, B*, 2018, **271**, 157–163.
- 63 Y. Li, D.-G. Cai, Z.-H. Zhu, H. Xu, T.-F. Zheng, J.-L. Chen, S.-J. Liu and H.-R. Wen, Solvothermal synthesis and device fabrication of a Eu<sup>3+</sup>-based metal–organic framework as a turn-on and blue-shift fluorescence sensor toward Cr<sup>3+</sup>, Al<sup>3+</sup> and Ga<sup>3+</sup>, *Dalton Trans.*, 2023, **52**(13), 4167–4175.
- 64 T. L. H. Doan, T. Q. Dao, H. N. Tran, P. H. Tran and T. N. Le, An efficient combination of Zr-MOF and microwave irradiation in catalytic Lewis acid Friedel–Crafts benzoylation, *Dalton Trans.*, 2016, **45**(18), 7875–7880.
- 65 T. V. Tran, H. T. N. Le, H. Q. Ha, X. N. T. Duong, L. H. T. Nguyen, T. L. H. Doan, H. L. Nguyen and T. Truong, A five coordination Cu(II) cluster-based MOF and its application in the synthesis of pharmaceuticals via sp<sup>3</sup> C–H/N–H oxidative coupling, *Catal. Sci. Technol.*, 2017, **7**(16), 3453–3458.
- 66 D. Pedrero, C. Edo, F. Fernández-Piñas, R. Rosal and S. Aguado, Efficient removal of nanoplastics from water using mesoporous metal organic frameworks, *Sep. Purif. Technol.*, 2024, **333**, 125816.
- 67 Z. Gao, B. Li, Z. Li, T. Yu, S. Wang, Q. Fang, S. Qiu and M. Xue, Free-Standing Metal–Organic Framework Membranes Made by Solvent-Free Space-Confined Conversion for Efficient H<sub>2</sub>/CO<sub>2</sub> Separation, *ACS Appl. Mater. Interfaces*, 2023, **15**(15), 19241–19249.
- 68 L. H. T. Nguyen, T. T. T. Nguyen, Y. T. Dang, P. H. Tran and T. Le Hoang Doan, Microwave-assisted synthesis as an efficient method to enhance the catalytic activity of Zr-based metal organic framework UiO-66 in a heterocyclization reaction, *Asian J. Org. Chem.*, 2019, **8**(12), 2276–2281.
- 69 L. H. T. Nguyen, H. T. T. Nguyen, B. Q. G. Le, M.-H. D. Dang, T. T. T. Nguyen, N. X. D. Mai and T. L. H. Doan, Microwave-assisted solvothermal synthesis of defective zirconium-organic framework as a recyclable nano-adsorbent with superior adsorption capacity for efficient removal of toxic organic dyes, *Colloid Interface Sci. Commun.*, 2022, **46**, 100511.
- 70 Y. Dang, H. Hoang, H. Dong, K.-B. Bui, L. Nguyen, T. Phan, Y. Kawazoe and T. Doan, Microwave-assisted Synthesis of Nano Hf- and Zr-based Metal–Organic Frameworks for Enhancement of Curcumin Adsorption, *Microporous Mesoporous Mater.*, 2020, **298**, 110064.
- 71 L. H. T. Nguyen, T. T. T. Nguyen, M.-H. D. Dang, P. H. Tran and T. L. H. Doan, Heterocyclic reaction induced by Brønsted–Lewis dual acidic Hf-MOF under microwave irradiation, *Mol. Catal.*, 2021, **499**, 111291.
- 72 M. Wen, N. Sun, L. Jiao, S. Q. Zang and H. L. Jiang, Microwave-Assisted Rapid Synthesis of MOF-Based Single-Atom Ni Catalyst for CO<sub>2</sub> Electroreduction at Ampere-Level Current, *Angew. Chem.*, 2024, **136**(10), e202318338.
- 73 X. Wu, Z. Bao, B. Yuan, J. Wang, Y. Sun, H. Luo and S. Deng, Microwave synthesis and characterization of MOF-74 (M = Ni, Mg) for gas separation, *Microporous Mesoporous Mater.*, 2013, **180**, 114–122.
- 74 C. Carrillo-Carrión, J. Farrando-Perez, L. L. Daemen, Y. Q. Cheng, A. J. Ramirez-Cuesta and J. Silvestre-Albero, Zr-Porphyrin Metal–Organic Framework as nanoreactor for boosting the formation of hydrogen clathrates, *Angew. Chem.*, 2024, **136**(6), e202315280.
- 75 T. T. T. Nguyen, B. Q. G. Le, V. T. H. Nguyen, J. H. Lee, N. X. D. Mai, L. H. T. Nguyen and T. L. H. Doan, Microwave-Assisted Synthesis of Porous Biomolecule-Incorporated Metal–Organic Frameworks as Efficient Nanocarriers for Anti-Cancer Drugs, *ChemistrySelect*, 2023, **8**(25), e202301543.
- 76 L. N. Appelhans, L. Hughes, B. McKenzie, M. Rodriguez, J. Griego, J. Briscoe, M. Moorman, E. Frederick and J. B. Wright, Facile microwave synthesis of zirconium metal-organic framework thin films on gold and silicon and application to sensor functionalization, *Microporous Mesoporous Mater.*, 2021, **323**, 111133.
- 77 P. Tapangpan, K. Panyarat, C. Chankaew, K. Grudpan and A. Rujiwatra, Terbium metal organic framework: microwave synthesis and selective sensing of nitrite, *Inorg. Chem. Commun.*, 2020, **111**, 107627.
- 78 I. Thomas-Hillman, A. Laybourn, C. Dodds and S. W. Kingman, Realising the environmental benefits of metal-organic frameworks: recent advances in microwave synthesis, *J. Mater. Chem. A*, 2018, **6**(25), 11564–11581.
- 79 T. J. Azbell, T. A. Pitt, M. M. Bollmeyer, C. Cong, K. M. Lancaster and P. J. Milner, Ionothermal Synthesis of Metal–Organic Frameworks Using Low-Melting Metal Salt Precursors, *Angew. Chem., Int. Ed.*, 2023, **62**(17), e202218252.
- 80 Q.-Y. Liu, Y.-L. Wang, N. Zhang, Y.-L. Jiang, J.-J. Wei and F. Luo, Spontaneous resolution in the ionothermal synthesis of homochiral Zn (II) metal–organic frameworks with (10, 3)-a topology constructed from achiral 5-sulfoisophthalate, *Cryst. Growth Des.*, 2011, **11**(9), 3717–3720.
- 81 K. Lu, A. Liebman Pelaez, L.-C. Wu, Y. Cao, C.-H. Zhu and H. Fu, Ionothermal synthesis of five keggin-type polyoxometalate-based metal–organic frameworks, *Inorg. Chem.*, 2019, **58**(3), 1794–1805.
- 82 M. Teixeira, R. A. Maia, L. Karmazin, B. Louis and S. A. Baudron, Ionothermal synthesis of calcium-based metal–organic frameworks in a deep eutectic solvent, *CrystEngComm*, 2022, **24**(3), 601–608.
- 83 P. Li, F.-F. Cheng, W.-W. Xiong and Q. Zhang, New synthetic strategies to prepare metal–organic frameworks, *Inorg. Chem. Front.*, 2018, **5**(11), 2693–2708.
- 84 W. Li, W. Xiao, Q. Luo, J. Yan, G. Zhang, L. Chen and J. Sun, Ionic liquids promoted synthesis, enhanced functions, and expanded applications of porous organic frameworks, *Coord. Chem. Rev.*, 2023, **493**, 215304.
- 85 B. Y. Xia, Y. Yan, N. Li, H. B. Wu, X. W. D. Lou and X. Wang, A metal–organic framework-derived bifunctional oxygen electrocatalyst, *Nat. Energy*, 2016, **1**(1), 1–8.
- 86 T. Huang, Y. Chen and J.-M. Lee, Two-dimensional cobalt/N-doped carbon hybrid structure derived from metal–organic frameworks as efficient electrocatalysts for hydrogen evolution, *ACS Sustainable Chem. Eng.*, 2017, **5**(7), 5646–5650.
- 87 J. Li, Q. Wu, X. Wang, B. Wang and T. Liu, Metal-organic framework-derived Co/CoO nanoparticles with tunable

- particle size for strong low-frequency microwave absorption in the S and C bands, *J. Colloid Interface Sci.*, 2022, **628**, 10–21.
- 88 W. Wang, X. Xu, W. Zhou and Z. Shao, Recent progress in metal-organic frameworks for applications in electrocatalytic and photocatalytic water splitting, *Adv. Sci.*, 2017, **4**(4), 1600371.
- 89 S. Główniak, B. Szczeńśniak, J. Choma and M. Jaroniec, Mechanochemistry: Toward green synthesis of metal-organic frameworks, *Mater. Today*, 2021, **46**, 109–124.
- 90 A. Metaweia, R. Soto, M. Khraisheh, G. Walker and A. B. Albadarin, Application of Raman and chemometrics to the mechanochemical synthesis of 4, 4-bipyridine/cobalt based MOF using twin screw extrusion, *Powder Technol.*, 2024, **437**, 119558.
- 91 D. Chen, J. Zhao, P. Zhang and S. Dai, Mechanochemical synthesis of metal-organic frameworks, *Polyhedron*, 2019, **162**, 59–64.
- 92 H. Ren and T. Wei, Electrochemical synthesis methods of metal-organic frameworks and their environmental analysis applications: a review, *ChemElectroChem*, 2022, **9**(13), e202200196.
- 93 L. Wu, M. Zhao, Q. Ye, X. Xin, K. Zhang, Y. Chen and Z. Wang, Electrochemical synthesis of ultra-flexible PES/HKUST-1 composite membranes for wastewater treatment, *Microporous Mesoporous Mater.*, 2024, **366**, 112917.
- 94 Y. Liu, Y. Wei, M. Liu, Y. Bai, X. Wang, S. Shang, J. Chen and Y. Liu, Electrochemical Synthesis of Large Area Two-Dimensional Metal-Organic Framework Films on Copper Anodes, *Angew. Chem., Int. Ed.*, 2021, **60**(6), 2887–2891.
- 95 C. Lu, T. Ben, S. Xu and S. Qiu, Electrochemical synthesis of a microporous conductive polymer based on a metal-organic framework thin film, *Angew. Chem.*, 2014, **126**(25), 6572–6576.
- 96 S. Jabarian and A. Ghaffarinejad, Electrochemical synthesis of NiBTC metal organic framework thin layer on nickel foam: an efficient electrocatalyst for the hydrogen evolution reaction, *J. Inorg. Organomet. Polym. Mater.*, 2019, **29**, 1565–1574.
- 97 Z. Ye, Y. Jiang, L. Li, F. Wu and R. Chen, MOF-related electrocatalysts for sulfur reduction/evolution reactions: Composition modulation, structure design, and mechanism research, *eScience*, 2023, **3**(5), 100107.
- 98 A. Asghar, N. Iqbal, T. Noor, B. M. Kariuki, L. Kidwell and T. L. Easun, Efficient electrochemical synthesis of a manganese-based metal-organic framework for H<sub>2</sub> and CO<sub>2</sub> uptake, *Green Chem.*, 2021, **23**(3), 1220–1227.
- 99 S. Zhou, O. Shekhah, J. Jia, J. Czaban-Jóźwiak, P. M. Bhatt, A. Ramírez, J. Gascon and M. Eddaoudi, Electrochemical synthesis of continuous metal-organic framework membranes for separation of hydrocarbons, *Nat. Energy*, 2021, **6**(9), 882–891.
- 100 F. Zhang, T. Zhang, X. Zou, X. Liang, G. Zhu and F. Qu, Electrochemical synthesis of metal organic framework films with proton conductive property, *Solid State Ionics*, 2017, **301**, 125–132.
- 101 H. Yuan, J. Cui, N. Li, M. Li, X. Yu, W. Fan, A. Karmakar, J. Dong, S. J. Pennycook and H. Cai, On-chip template-directed conversion of metal hydroxides to metal-organic framework films with enhanced adhesion, *ACS Appl. Mater. Interfaces*, 2020, **12**(32), 36715–36722.
- 102 W. Liu, Y. Yang, X. Yang, Y.-L. Peng, P. Cheng, Z. Zhang and Y. Chen, Template-directed fabrication of highly efficient metal-organic framework photocatalysts, *ACS Appl. Mater. Interfaces*, 2021, **13**(49), 58619–58629.
- 103 Y. Yang, D. Cong and S. Hao, Template-Directed Ordered Mesoporous Silica@ Palladium-Containing Zinc Metal-Organic Framework Composites as Highly Efficient Suzuki Coupling Catalysts, *ChemCatChem*, 2016, **8**(5), 900–905.
- 104 H. Huang, J.-R. Li, K. Wang, T. Han, M. Tong, L. Li, Y. Xie, Q. Yang, D. Liu and C. Zhong, An in situ self-assembly template strategy for the preparation of hierarchical-pore metal-organic frameworks, *Nat. Commun.*, 2015, **6**(1), 8847.
- 105 L. Meng, B. Yu and Y. Qin, Templated interfacial synthesis of metal-organic framework (MOF) nano- and microstructures with precisely controlled shapes and sizes, *Commun. Chem.*, 2021, **4**(1), 82.
- 106 R. Fan, N. Kang, Y. Li and L. Gao, A template-directed synthesis of metal-organic framework (MOF-74) ultrathin nanosheets for oxygen reduction electrocatalysis, *RSC Adv.*, 2021, **11**(16), 9353–9360.
- 107 X. Yang, T. Liang, J. Sun, M. J. Zaworotko, Y. Chen, P. Cheng and Z. Zhang, Template-Directed Synthesis of Photocatalyst-Encapsulating Metal-Organic Frameworks with Boosted Photocatalytic Activity, *ACS Catal.*, 2019, **9**(8), 7486–7493.
- 108 B. Ding, J. Wang, Z. Chang, G. Xu, X. Hao, L. Shen, H. Dou and X. Zhang, Self-Sacrificial Template-Directed Synthesis of Metal-Organic Framework-Derived Porous Carbon for Energy-Storage Devices, *ChemElectroChem*, 2016, **3**(4), 668–674.
- 109 S. Li, M. Dharmawardana, R. P. Welch, Y. Ren, C. M. Thompson, R. A. Smaldone and J. J. Gassensmith, Template-directed synthesis of porous and protective core-shell bionanoparticles, *Angew. Chem., Int. Ed.*, 2016, **55**(36), 10691–10696.
- 110 M. Kim, M. Pander and H. R. Moon, Advancing Metal-Organic Framework Designs for Room-Temperature Chemiresistive Gas Sensors, *ACS Appl. Electron. Mater.*, 2024, **6**(5), 3024–3038.
- 111 R. Zhang, L. Lu, Y. Chang and M. Liu, Gas sensing based on metal-organic frameworks: Concepts, functions, and developments, *J. Hazard. Mater.*, 2022, **429**, 128321.
- 112 X. Peng, X. Wu, M. Zhang and H. Yuan, Metal-organic framework coated devices for gas sensing, *ACS Sen.*, 2023, **8**(7), 2471–2492.
- 113 J. Hao, X. Xu, H. Fei, L. Li and B. Yan, Functionalization of metal-organic frameworks for photoactive materials, *Adv. Mater.*, 2018, **30**(17), 1705634.
- 114 S. A. A. Razavi and A. Morsali, Linker functionalized metal-organic frameworks, *Coord. Chem. Rev.*, 2019, **399**, 213023.
- 115 B. T. Nguyen, H. L. Nguyen, T. C. Nguyen, K. E. Cordova and H. Furukawa, High Methanol Uptake Capacity in Two

- New Series of Metal–Organic Frameworks: Promising Materials for Adsorption-Driven Heat Pump Applications, *Chem. Mater.*, 2016, **28**(17), 6243–6249.
- 116 H. L. Nguyen, R. Matheu, C. S. Diercks, T. L. Doan, B. T. Nguyen and K. E. Cordova, Postsynthetic metalation of a new metal–organic framework to improve methane working storage capacity, *ACS Mater. Lett.*, 2022, **4**(11), 2375–2380.
- 117 T. M. T. Le, N. T. T. Nguyen, N. M. Q. Tran, Q. T. Pham, T. M. Le, L. D. Nguyen, P. H. Tran, T. L. H. Doan and L. H. T. Nguyen, Post-synthesis of curcumin-embedded zeolitic imidazole framework for copper ions detection, *J. Porous Mater.*, 2024, 1–14.
- 118 S. Mandal, S. Natarajan, P. Mani and A. Pankajakshan, Post-synthetic modification of metal–organic frameworks toward applications, *Adv. Funct. Mater.*, 2021, **31**(4), 2006291.
- 119 L. H. Nguyen, H. L. Nguyen, T. L. Doan and P. H. Tran, A new superacid hafnium-based metal–organic framework as a highly active heterogeneous catalyst for the synthesis of benzoxazoles under solvent-free conditions, *Catal. Sci. Technol.*, 2017, **7**(19), 4346–4350.
- 120 R. Thür, N. Van Velthoven, V. Lemmens, M. Bastin, S. Smolders, D. De Vos and I. F. Vankelecom, Modulator-mediated functionalization of MOF-808 as a platform tool to create high-performance mixed-matrix membranes, *ACS Appl. Mater. Interfaces*, 2019, **11**(47), 44792–44801.
- 121 Y. Liu, Y.-K. Lu, B. Zhang, L. Hou and Y.-Y. Wang, Post-synthetic functionalization of Ni-MOF by Eu<sup>3+</sup> ions: luminescent probe for aspartic acid and magnetic property, *Inorg. Chem.*, 2020, **59**(11), 7531–7538.
- 122 Y. T. Dang, M.-H. D. Dang, N. X. D. Mai, L. H. T. Nguyen, T. B. Phan, H. V. Le and T. L. H. Doan, Room temperature synthesis of biocompatible nano Zn-MOF for the rapid and selective adsorption of curcumin, *J. Sci.: Adv. Mater. Devices*, 2020, **5**(4), 560–565.
- 123 L. H. T. Nguyen, M.-T. Le Nguyen, T. N. Ha, H. T. Hoang, N. K. Pham, Y. Kawazoe, D. Nguyen-Manh and T. L. H. Doan, Engineering functionalized Zr-MOFs as facile removal of indole: Experimental studies and first-principles modeling, *J. Sci.: Adv. Mater. Devices*, 2024, **9**(1), 100661.
- 124 D. E. Vanpoucke, Linker functionalization in MIL-47 (V)-R metal–organic frameworks: understanding the electronic structure, *J. Phys. Chem. C*, 2017, **121**(14), 8014–8022.
- 125 M.-H. D. Dang, L. H. T. Nguyen, T. T. T. Nguyen, N. X. D. Mai, P. H. Tran and T. L. H. Doan, Using sulfate-functionalized Hf-based metal–organic frameworks as a heterogeneous catalyst for solvent-free synthesis of pyrimido [1, 2-a] benzimidazoles via one-pot three-component reaction, *J. Ind. Eng. Chem.*, 2021, **103**, 340–347.
- 126 S. Dissegna, K. Epp, W. R. Heinz, G. Kieslich and R. A. Fischer, Defective metal-organic frameworks, *Adv. Mater.*, 2018, **30**(37), 1704501.
- 127 W. Xiang, Y. Zhang, Y. Chen, C.-J. Liu and X. Tu, Synthesis, characterization and application of defective metal–organic frameworks: current status and perspectives, *J. Mater. Chem. A*, 2020, **8**(41), 21526–21546.
- 128 X. Ma, L. Wang, Q. Zhang and H. L. Jiang, Switching on the photocatalysis of metal–organic frameworks by engineering structural defects, *Angew. Chem., Int. Ed.*, 2019, **58**(35), 12175–12179.
- 129 D. T. Nguyen, L. D. T. Nguyen, Q. T. Pham, T. M. Le, B. Q. G. Le, N. X. D. Mai, T. L. H. Doan and L. H. T. Nguyen, Zeolitic imidazolate frameworks as an efficient platform for potential curcumin-based on/off fluorescent chemosensor, *Microporous Mesoporous Mater.*, 2021, **327**, 111445.
- 130 J.-H. Lee, T. T. T. Nguyen, L. H. T. Nguyen, T. B. Phan, S. S. Kim and T. L. H. Doan, Functionalization of zirconium-based metal–organic frameworks for gas sensing applications, *J. Hazard. Mater.*, 2021, **403**, 124104.
- 131 T. T. T. Nguyen, B. Q. G. Le, M.-H. D. Dang, B. T. Phan, N. X. D. Mai and T. L. H. Doan, Facile synthesis of novel fluorescent organosilica-coated MOF nanoparticles for fast curcumin adsorption, *Microporous Mesoporous Mater.*, 2022, **338**, 111944.
- 132 S. Li, M. Dharmarwardana, R. Welch, Y. Ren, C. Thompson, R. Smaldone and J. Gassensmith, Template-Directed Synthesis of Porous and Protective Core-Shell Bionanoparticles, *Angew. Chem.*, 2016, **128**, 10849–10854.
- 133 S. Wang, W. Morris, Y. Liu, C. M. McGuirk, Y. Zhou, J. T. Hupp, O. K. Farha and C. A. Mirkin, Surface-specific functionalization of nanoscale metal–organic frameworks, *Angew. Chem., Int. Ed.*, 2015, **54**(49), 14738–14742.
- 134 S. Darvishi, S. Sadjadi, E. Monflier, A. Heydari and M. M. Heravi, Sulfonic acid-functionalized k-carrageenan/Cr-based metal-organic framework: An efficient and recyclable catalyst for fructose conversion to 5-hydroxymethylfurfural, *Int. J. Biol. Macromol.*, 2024, **264**, 130555.
- 135 Y. Fang, Y. Ma, M. Zheng, P. Yang, A. M. Asiri and X. Wang, Metal–organic frameworks for solar energy conversion by photoredox catalysis, *Coord. Chem. Rev.*, 2018, **373**, 83–115.
- 136 M. S. Khan, Y. Li, D.-S. Li, J. Qiu, X. Xu and H. Y. Yang, A review of metal–organic framework (MOF) materials as an effective photocatalyst for degradation of organic pollutants, *Nanoscale Adv.*, 2023, **5**(23), 6318–6348.
- 137 M. Hefayathullah, S. Singh, V. Ganesan and G. Maduraiveeran, Metal-organic frameworks for biomedical applications: A review, *Adv. Colloid Interface Sci.*, 2024, **331**, 103210.
- 138 S.-J. Fan, J. Heinrich, M. S. Bloom, T.-Y. Zhao, T.-X. Shi, W.-R. Feng, Y. Sun, J.-C. Shen, Z.-C. Yang and B.-Y. Yang, Ambient air pollution and depression: a systematic review with meta-analysis up to 2019, *Sci. Total Environ.*, 2020, **701**, 134721.
- 139 D. A. Glencross, T.-R. Ho, N. Camina, C. M. Hawrylowicz and P. E. Pfeffer, Air pollution and its effects on the immune system, *Free Radicals Biol. Med.*, 2020, **151**, 56–68.
- 140 K. Wetchakun, T. Samerjai, N. Tamaekong, C. Liewhiran, C. Siri Wong, V. Kruefu, A. Wisitorsaat, A. Tuantranont and S. Phanichphant, Semiconducting metal oxides as sensors for environmentally hazardous gases, *Sens. Actuators, B*, 2011, **160**(1), 580–591.
- 141 P. Wu, Q. Guo, Y. Zhao, M. Bian, S. Cao, J. J. Zhang and X. Duan, Emerging concern on air pollution and health:

- Trade-off between air pollution exposure and physical activity, *Eco-Environ. Health*, 2024, 3(2), 202–207.
- 142 M. Kampa and E. Castanas, Human health effects of air pollution, *Environ. Pollut.*, 2008, 151(2), 362–367.
- 143 I. Manisalidis, E. Stavropoulou, A. Stavropoulos and E. Bezirtzoglou, Environmental and health impacts of air pollution: a review, *Front. Public Health*, 2020, 8, 14.
- 144 R. M. Babadjouni, D. M. Hodis, R. Radwanski, R. Durazo, A. Patel, Q. Liu and W. J. Mack, Clinical effects of air pollution on the central nervous system; a review, *J. Clin. Neurosci.*, 2017, 43, 16–24.
- 145 J. G. Lu, Air pollution: A systematic review of its psychological, economic, and social effects, *Curr. Opin. Psychol.*, 2020, 32, 52–65.
- 146 C. Li, X. Xia, Y. Lin and H. Wen, Polluted cognition: The effect of air pollution on online purchasing behavior, *J. Retail. Consum. Serv.*, 2024, 79, 103839.
- 147 K. Liu, H. Zhang, Y. Bo, Y. Chen, P. Zhang, C. Huang, Z. Yu and Z. Gao, Ambient air pollution and Children's health: An umbrella review, *Atmos. Pollut. Res.*, 2024, 102108.
- 148 A. Mirzaei, H. R. Ansari, M. Shahbaz, J.-Y. Kim, H. W. Kim and S. S. Kim, Metal oxide semiconductor nanostructure gas sensors with different morphologies, *Chemosensors*, 2022, 10(7), 289.
- 149 A. M. Kotecha, A. D. Corrêa, K. M. Fisher and J. V. Rushworth, Olfactory dysfunction as a global biomarker for sniffing out Alzheimer's disease: a meta-analysis, *Bio-sensors*, 2018, 8(2), 41.
- 150 A. Mirzaei, S. S. Kim and H. W. Kim, Resistance-based H<sub>2</sub>S gas sensors using metal oxide nanostructures: A review of recent advances, *J. Hazard. Mater.*, 2018, 357, 314–331.
- 151 A. Nasri, M. Petrissans, V. Fierro and A. Celzard, Gas sensing based on organic composite materials: Review of sensor types, progresses and challenges, *Mater. Sci. Semi-cond. Process.*, 2021, 128, 105744.
- 152 L. Hao, W. Ruijie, L. Hua-Bin, H. Li-Ying, Y. Wen-Jing, H. Zhong-Qiu, S.-R. Fan and W. Yi, A novel catalytic-type gas sensor based on alumina ceramic substrates loaded with catalysts and printed electrodes, *Chin. J. Anal. Chem.*, 2021, 49(11), 93–101.
- 153 A. Mirzaei, J.-H. Kim, H. W. Kim and S. S. Kim, Gasochromic WO<sub>3</sub> nanostructures for the detection of hydrogen gas: An overview, *Appl. Sci.*, 2019, 9(9), 1775.
- 154 A. H. Ismail and Y. Sulaiman, Review on the utilisation of sensing materials for intrinsic optical NH<sub>3</sub> gas sensors, *Synth. Met.*, 2021, 280, 116860.
- 155 G. Korotcenkov, S. D. Han and J. R. Stetter, Review of electrochemical hydrogen sensors, *Chem. Rev.*, 2009, 109(3), 1402–1433.
- 156 Z. Zhai, X. Zhang, X. Hao, B. Niu and C. Li, Metal–organic frameworks materials for capacitive gas sensors, *Adv. Mater. Technol.*, 2021, 6(10), 2100127.
- 157 A. Singh, N. Chowdhury, S. C. Roy and B. Bhowmik, Review of thin film transistor gas sensors: Comparison with resistive and capacitive sensors, *J. Electron. Mater.*, 2022, 51(5), 1974–2003.
- 158 E. H. Kwon, M. Kim, C. Y. Lee, M. Kim and Y. D. Park, Metal–organic-framework-decorated carbon nanofibers with enhanced gas sensitivity when incorporated into an organic semiconductor-based gas sensor, *ACS Appl. Mater. Interfaces*, 2022, 14(8), 10637–10647.
- 159 S. Fanget, S. Hentz, P. Puget, J. Arcamone, M. Matheron, E. Colinet, P. Andreucci, L. Duraffourg, E. Myers and M. Roukes, Gas sensors based on gravimetric detection—A review, *Sens. Actuators, B*, 2011, 160(1), 804–821.
- 160 Z. Li, Z. Yao, A. A. Haidry, T. Plecenik, L. Xie, L. Sun and Q. Fatima, Resistive-type hydrogen gas sensor based on TiO<sub>2</sub>: A review, *Int. J. Hydrogen Energy*, 2018, 43(45), 21114–21132.
- 161 S. M. Majhi, A. Mirzaei, H. W. Kim, S. S. Kim and T. W. Kim, Recent advances in energy-saving chemiresistive gas sensors: A review, *Nano Energy*, 2021, 79, 105369.
- 162 A. Mirzaei, S. Leonardi and G. Neri, Detection of hazardous volatile organic compounds (VOCs) by metal oxide nanostructures-based gas sensors: A review, *Ceram. Int.*, 2016, 42(14), 15119–15141.
- 163 V. Amiri, H. Roshan, A. Mirzaei, G. Neri and A. I. Ayesh, Nanostructured metal oxide-based acetone gas sensors: A review, *Sensors*, 2020, 20(11), 3096.
- 164 Y. Masuda, Recent advances in SnO<sub>2</sub> nanostructure based gas sensors, *Sens. Actuators, B*, 2022, 364, 131876.
- 165 M. A. Franco, P. P. Conti, R. S. Andre and D. S. Correa, A review on chemiresistive ZnO gas sensors, *Sens. Actuators Rep.*, 2022, 4, 100100.
- 166 M. Wusiman and F. Taghipour, Methods and mechanisms of gas sensor selectivity, *Crit. Rev. Solid State Mater. Sci.*, 2022, 47(3), 416–435.
- 167 X. Huang, Z. Gong and Y. Lv, Advances in metal-organic frameworks-based gas sensors for hazardous substances, *TrAC, Trends Anal. Chem.*, 2022, 153, 116644.
- 168 S. Chen, X. Duan, C. Liu, S. Liu, P. Li, D. Su, X. Sun, Y. Guo, W. Chen and Z. Wang, La-Ce-MOF nanocomposite coated quartz crystal microbalance gas sensor for the detection of amine gases and formaldehyde, *J. Hazard. Mater.*, 2024, 467, 133672.
- 169 S. G. Surya, S. Bhanoth, S. M. Majhi, Y. D. More, V. M. Teja and K. N. Chappanda, A silver nanoparticle-anchored UiO-66 (Zr) metal–organic framework (MOF)-based capacitive H<sub>2</sub>S gas sensor, *CrystEngComm*, 2019, 21(47), 7303–7312.
- 170 H. Sohrabi, S. Ghasemzadeh, Z. Ghoreishi, M. R. Majidi, Y. Yoon, N. Dizge and A. Khataee, Metal-organic frameworks (MOF)-based sensors for detection of toxic gases: A review of current status and future prospects, *Mater. Chem. Phys.*, 2023, 299, 127512.
- 171 Y. M. Jo, Y. K. Jo, J. H. Lee, H. W. Jang, I. S. Hwang and D. J. Yoo, MOF-based chemiresistive gas sensors: toward new functionalities, *Adv. Mater.*, 2023, 35(43), 2206842.
- 172 S. M. Majhi, A. Ali, P. Rai, Y. E. Greish, A. Alzamy, S. G. Surya, N. Qamhieh and S. T. Mahmoud, Metal–organic frameworks for advanced transducer based gas sensors: review and perspectives, *Nanoscale Adv.*, 2022, 4(3), 697–732.

- 173 X. Zhang, S. Zhang, Y. Tang, X. Huang and H. Pang, Recent advances and challenges of metal–organic framework/graphene-based composites, *Composites, Part B*, 2022, **230**, 109532.
- 174 L. J. Small, M. E. Schindelholz and T. M. Nenoff, Hold on tight: MOF-based irreversible gas sensors, *Ind. Eng. Chem. Res.*, 2021, **60**(21), 7998–8006.
- 175 L. Chen, X. Zhang, X. Cheng, Z. Xie, Q. Kuang and L. Zheng, The function of metal–organic frameworks in the application of MOF-based composites, *Nanoscale Adv.*, 2020, **2**(7), 2628–2647.
- 176 L. E. Kreno, K. Leong, O. K. Farha, M. Allendorf, R. P. Van Duyne and J. T. Hupp, Metal–organic framework materials as chemical sensors, *Chem. Rev.*, 2012, **112**(2), 1105–1125.
- 177 X.-F. Wang, X.-Z. Song, K.-M. Sun, L. Cheng and W. Ma, MOFs-derived porous nanomaterials for gas sensing, *Polyhedron*, 2018, **152**, 155–163.
- 178 H. Wei, H. Zhang, B. Song, K. Yuan, H. Xiao, Y. Cao and Q. Cao, Metal–Organic Framework (MOF) derivatives as promising chemiresistive gas sensing materials: A Review, *Int. J. Environ. Res. Public Health*, 2023, **20**(5), 4388.
- 179 H. Yuan, N. Li, W. Fan, H. Cai and D. Zhao, Metal-organic framework based gas sensors, *Adv. Sci.*, 2022, **9**(6), 2104374.
- 180 M. Drobek, J.-H. Kim, M. Bechelany, C. Vallicari, A. Julbe and S. S. Kim, MOF-Based Membrane Encapsulated ZnO Nanowires for Enhanced Gas Sensor Selectivity, *ACS Appl. Mater. Interfaces*, 2016, **8**(13), 8323–8328.
- 181 M.-S. Yao, L.-A. Cao, Y.-X. Tang, G.-E. Wang, R.-H. Liu, P. N. Kumar, G.-D. Wu, W.-H. Deng, W.-J. Hong and G. Xu, Gas transport regulation in a MO/MOF interface for enhanced selective gas detection, *J. Mater. Chem. A*, 2019, **7**(31), 18397–18403.
- 182 Z. Wang, L. Zhu, J. Wang, R. Zhuang, P. Mu, J. Wang and W. Yan, Advances in functional guest materials for resistive gas sensors, *RSC Adv.*, 2022, **12**(38), 24614–24632.
- 183 X. Zhuang, S. Zhang, Y. Tang, F. Yu, Z. Li and H. Pang, Recent progress of MOF/MXene-based composites: synthesis, functionality and application, *Coord. Chem. Rev.*, 2023, **490**, 215208.
- 184 H. Shiozawa, B. C. Bayer, H. Peterlik, J. C. Meyer, W. Lang and T. Pichler, Doping of metal–organic frameworks towards resistive sensing, *Sci. Rep.*, 2017, **7**(1), 2439.
- 185 H.-Y. Li, S.-N. Zhao, S.-Q. Zang and J. Li, Functional metal–organic frameworks as effective sensors of gases and volatile compounds, *Chem. Soc. Rev.*, 2020, **49**(17), 6364–6401.
- 186 C. Arul, K. Moulae, N. Donato, D. Iannazzo, N. Lavanya, G. Neri and C. Sekar, Temperature modulated Cu-MOF based gas sensor with dual selectivity to acetone and NO<sub>2</sub> at low operating temperatures, *Sens. Actuators, B*, 2021, **329**, 129053.
- 187 W.-T. Koo, H.-J. Cho, D.-H. Kim, Y. H. Kim, H. Shin, R. M. Penner and I.-D. Kim, Chemiresistive hydrogen sensors: fundamentals, recent advances, and challenges, *ACS Nano*, 2020, **14**(11), 14284–14322.
- 188 J. Baeyens, H. Zhang, J. Nie, L. Appels, R. Dewil, R. Ansart and Y. Deng, Reviewing the potential of bio-hydrogen production by fermentation, *Renewable Sustainable Energy Rev.*, 2020, **131**, 110023.
- 189 Q. Zhang, H. Yang, T. Zhou, X. Chen, W. Li and H. Pang, Metal–organic frameworks and their composites for environmental applications, *Adv. Sci.*, 2022, **9**(32), 2204141.
- 190 M. A. Deshmukh, M. D. Shirsat, A. Ramanaviciene and A. Ramanavicius, Composites based on conducting polymers and carbon nanomaterials for heavy metal ion sensing, *Crit. Rev. Anal. Chem.*, 2018, **48**(4), 293–304.
- 191 A. Mirzaei, S. P. Bharath, J.-Y. Kim, K. K. Pawar, H. W. Kim and S. S. Kim, N-Doped Graphene and its derivatives as resistive gas sensors: An overview, *Chemosensors*, 2023, **11**(6), 334.
- 192 C. Wang, Y. Wang, Z. Yang and N. Hu, Review of recent progress on graphene-based composite gas sensors, *Ceram. Int.*, 2021, **47**(12), 16367–16384.
- 193 S. M. Majhi, A. Mirzaei, H. W. Kim and S. S. Kim, Reduced graphene oxide (rGO)-loaded metal-oxide nanofiber gas sensors: An overview, *Sensors*, 2021, **21**(4), 1352.
- 194 M. S. More, G. A. Bodkhe, N. N. Ingle, F. Singh, M.-L. Tsai, M. Kim and M. D. Shirsat, Metal-organic framework (MOF)/reduced graphene oxide (rGO) composite for high performance CO sensor, *Solid-State Electron.*, 2023, **204**, 108638.
- 195 C. Gao, T. Wang, X. Wang and A. NH<sub>3</sub>, Gas Sensor Based on Flexible Copper (II) isonicotinate MOF/Reduced Graphene Oxide Composite Modified Interdigital Electrode, *Int. J. Electrochem. Sci.*, 2022, **17**(7), 220763.
- 196 K. Jayaramulu, M. E. DMello, K. Kesavan, A. Schneemann, M. Otyepka, S. Kment, C. Narayana, S. B. Kalidindi, R. S. Varma and R. Zboril, A multifunctional covalently linked graphene–MOF hybrid as an effective chemiresistive gas sensor, *J. Mater. Chem. A*, 2021, **9**(32), 17434–17441.
- 197 Y. Yuan, J. Chen, K. Polat and A. Alhudhaif, An innovative approach to detecting the freshness of fruits and vegetables through the integration of convolutional neural networks and bidirectional long short-term memory network, *Curr. Res. Food Sci.*, 2024, **8**, 100723.
- 198 Q. Zhao, Z. Duan, Z. Yuan, X. Li, W. Si, B. Liu, Y. Zhang, Y. Jiang and H. Tai, High performance ethylene sensor based on palladium-loaded tin oxide: Application in fruit quality detection, *Chin. Chem. Lett.*, 2020, **31**(8), 2045–2049.
- 199 H. R. Ansari, A. Mirzaei, H. Shokrollahi, R. Kumar, J.-Y. Kim, H. W. Kim, M. Kumar and S. S. Kim, Flexible/wearable resistive gas sensors based on 2D materials, *J. Mater. Chem. C*, 2023, **11**(20), 6528–6549.
- 200 S. Li, X. Hu, S. Chen, X. Wang, H. Shang, Y. Zhou, J. Dai, L. Xiao, W. Qin and Y. Liu, Synthesis of  $\gamma$ -cyclodextrin metal-organic framework as ethylene absorber for improving postharvest quality of kiwi fruit, *Food Hydrocolloids*, 2023, **136**, 108294.
- 201 J. Chai, B. Liao, R. Li and Z. Liu, Changes in taste and volatile compounds and ethylene production determined

- the eating window of 'Xuxiang' and 'Cuixiang' kiwifruit cultivars, *Postharvest Biol. Technol.*, 2022, **194**, 112093.
- 202 H. Yan, J. Wang, N. Shi, Y. Han, S. Zhang and G. Zhao, A flexible and wearable chemiresistive ethylene gas sensor modified with PdNPs-SWCNTs@ Cu-MOF-74 nanocomposite: a targeted strategy for the dynamic monitoring of fruit freshness, *Chem. Eng. J.*, 2024, **488**, 151142.
- 203 P. Orellano, J. Reynoso and N. Quaranta, Short-term exposure to sulphur dioxide (SO<sub>2</sub>) and all-cause and respiratory mortality: A systematic review and meta-analysis, *Environ. Int.*, 2021, **150**, 106434.
- 204 N. Ingle, P. Sayyad, M. Deshmukh, G. Bodkhe, M. Mahadik, T. Al-Gahouari, S. Shirsat and M. D. Shirsat, A chemiresistive gas sensor for sensitive detection of SO<sub>2</sub> employing Ni-MOF modified-OH-SWNTs and-OH-MWNTs, *Appl. Phys. A: Mater. Sci. Process.*, 2021, **127**, 1–10.
- 205 I. Fratoddi, I. Venditti, C. Cametti and M. V. Russo, Chemiresistive polyaniline-based gas sensors: A mini review, *Sens. Actuators, B*, 2015, **220**, 534–548.
- 206 V. Kumar, A. Mirzaei, M. Bonyani, K.-H. Kim, H. W. Kim and S. S. Kim, Advances in electrospun nanofiber fabrication for polyaniline (PANI)-based chemoresistive sensors for gaseous ammonia, *TrAC, Trends Anal. Chem.*, 2020, **129**, 115938.
- 207 S. K. Bhardwaj, G. C. Mohanta, A. L. Sharma, K.-H. Kim and A. Deep, A three-phase copper MOF-graphene-polyaniline composite for effective sensing of ammonia, *Anal. Chim. Acta*, 2018, **1043**, 89–97.
- 208 L. V. Kayser and D. J. Lipomi, Stretchable conductive polymers and composites based on PEDOT and PEDOT:PSS, *Adv. Mater.*, 2019, **31**(10), 1806133.
- 209 G. Garg, N. Garg, A. Deep and D. Soni, Zr-MOF and PEDOT:PSS composite sensor for chemoresistive sensing of toluene at room temperature, *J. Alloys Compd.*, 2023, **956**, 170309.
- 210 A. Ali, H. H. ALTakroori, Y. E. Greish, A. Alzamy, L. A. Siddig, N. Qamhie and S. T. Mahmoud, Flexible Cu<sub>3</sub>(HHTP)<sub>2</sub> MOF membranes for gas sensing application at room temperature, *Nanomaterials*, 2022, **12**(6), 913.
- 211 B. Huang, Y. Li and W. Zeng, Application of metal-organic framework-based composites for gas sensing and effects of synthesis strategies on gas-sensitive performance, *Chemosensors*, 2021, **9**(8), 226.
- 212 D. Huang, P. Yong and S. Shen, MOF-decorated sea urchin-like In<sub>2</sub>O<sub>3</sub> gas sensor with higher gas sensitivity to formaldehyde, *J. Solid State Chem.*, 2023, **328**, 124336.
- 213 L. Fappiano, F. Carriera, A. Iannone, I. Notardonato and P. Avino, A review on recent sensing methods for determining formaldehyde in agri-food chain: A comparison with the conventional analytical approaches, *Foods*, 2022, **11**(9), 1351.
- 214 H. Salonen, T. Salthammer and L. Morawska, Human exposure to NO<sub>2</sub> in school and office indoor environments, *Environ. Int.*, 2019, **130**, 104887.
- 215 Y. Ogen, Assessing nitrogen dioxide (NO<sub>2</sub>) levels as a contributing factor to coronavirus (COVID-19) fatality, *Sci. Total Environ.*, 2020, **726**, 138605.
- 216 K. Y. Shin, L. H. T. Nguyen, H. L. Nguyen, A. Mirzaei, V. N. H. Tran, N. X. D. Mai, N. Q. Tran, W. Oum, E. B. Kim and H. M. Kim, Titanium-based metal-organic-framework-coated SnO<sub>2</sub> nanowires with enhanced NO<sub>2</sub> gas sensing capability in humid environment, *Sens. Actuators, B*, 2023, **394**, 134425.
- 217 J.-H. Kim, A. Mirzaei, H. W. Kim and S. S. Kim, Combination of Pd loading and electron beam irradiation for superior hydrogen sensing of electrospun ZnO nanofibers, *Sens. Actuators, B*, 2019, **284**, 628–637.
- 218 D. H. Yang, T. T. T. Nguyen, S. T. Navale, L. H. T. Nguyen, Y. T. Dang, N. X. D. Mai, T. B. Phan, J.-Y. Kim, T. L. H. Doan and S. S. Kim, Novel amine-functionalized zinc-based metal-organic framework for low-temperature chemiresistive hydrogen sensing, *Sens. Actuators, B*, 2022, **368**, 132120.
- 219 P. Goswami and G. Gupta, Recent progress of flexible NO<sub>2</sub> and NH<sub>3</sub> gas sensors based on transition metal dichalcogenides for room temperature sensing, *Materials Today, Chemistry*, 2022, **23**, 100726.
- 220 D. Kwak, Y. Lei and R. Maric, Ammonia gas sensors: A comprehensive review, *Talanta*, 2019, **204**, 713–730.
- 221 H.-Y. Li, C.-S. Lee, D. H. Kim and J.-H. Lee, Flexible room-temperature NH<sub>3</sub> sensor for ultrasensitive, selective, and humidity-independent gas detection, *ACS Appl. Mater. Interfaces*, 2018, **10**(33), 27858–27867.
- 222 M.-H. D. Dang, S. T. Navale, D. H. Yang, J.-Y. Kim, L. H. T. Nguyen, N. X. D. Mai, T. B. Phan, H. W. Kim, T. L. H. Doan and S. S. Kim, Sulfate-functionalized hafnium-organic frameworks as a highly effective chemiresistive sensor for low-temperature detection of hazardous NH<sub>3</sub> gas, *Sens. Actuators, B*, 2022, **367**, 132094.
- 223 J. A. Guzman, Carbon monoxide poisoning, *Crit. Care Clin.*, 2012, **28**(4), 537–548.
- 224 J. B. DeCoste, G. W. Peterson, H. Jasuja, T. G. Glover, Y.-G. Huang and K. S. Walton, Stability and degradation mechanisms of metal-organic frameworks containing the Zr<sub>6</sub>O<sub>4</sub>(OH)<sub>4</sub> secondary building unit, *J. Mater. Chem. A*, 2013, **1**(18), 5642–5650.
- 225 L. P. L. Mosca, A. B. Gapan, R. A. Angeles and E. C. R. Lopez, *Adv. Future Trends Eng. Proc.*, 2023, **56**(1), 146.
- 226 E. Namratha, T. Ghosh, S. Manabolu, A. Reddy, R. R. Gangavarapu and K. Suresh, Design and synthesis of M-TCPP@PVP (M = Ni, Zn) MOF composites for enhanced ammonia gas sensing and supercapacitor applications, *J. Mater. Sci.: Mater. Electron.*, 2024, 35.
- 227 J. Meng, X. Liu, C. Niu, Q. Pang, J. Li, F. Liu, Z. Liu and L. Mai, Advances in metal-organic framework coatings: versatile synthesis and broad applications, *Chem. Soc. Rev.*, 2020, **49**(10), 3142–3186.